Title
Cardiolipin in Barth Syndrome

Author
Ikon, Nikita

Publication Date
2017

Peer reviewed|Thesis/dissertation

Cardiolipin in Barth Syndrome

By

Nikita Ikon

A dissertation submitted in partial satisfaction

of the requirements for the degree of

Doctor of Philosophy

in

Metabolic Biology

in the

Graduate Division

of the

University of California, Berkeley

Committee in charge:
Professor Robert O. Ryan, Chair
Professor Jen-Chywan Wang
Professor James Olzmann
Professor George A. Brooks

Summer 2017

Abstract

Cardiolipin in Barth Syndrome

By

Nikita Ikon

Doctor of Philosophy in Metabolic biology

University of California, Berkeley

Professor Robert O. Ryan, Chair

Barth Syndrome (BTHS) is a rare genetic disorder caused by mutations in the gene that encodes tafazzin, a protein whose sole function is to remodel the mitochondrial phospholipid cardiolipin (CL). Despite comprising a small proportion of the body's total phospholipid pool, the critical role CL plays in the structure and function of the mitochondrial inner membrane means that defects in CL composition lead to profound mitochondrial impairment. These mitochondrial defects, in turn, lead to the failure of high energy-demand systems, resulting in neutropenia, skeletal muscle weakness, and cardiomyopathy. While some researchers have suggested gene therapy or protein replacement as potential future treatments, it is conceivable that, if CL could be delivered to the defective mitochondria, the need for a functional tafazzin could be bypassed entirely. In the current study, we use the amphipathic plasma protein apolipoprotein A-I to solubilize CL into discoidal nanoparticles resembling HDL. These CL nanodisks (CL-ND) were incubated with a cell culture model of the neutropenia seen in BTHS. CL-ND treatment increased cellular CL levels and ameliorated the BTHS phenotype. To extend these findings to whole animals, a 10 week study was carried out using a mouse model of BTHS. However, at the end of the study, while the BTHS mice developed significant differences in CL composition characteristic of the disease, CL-ND treatment had no effect on CL content or composition. Thus, while CL-ND may eventually prove to be a useful therapy for BTHS, the current study highlights the difficulty of translating cell culture results to intact animals.

Table of contents

Acknowledgements

Adapted, with permission, from Lipids, DOI: 10.1007/s11745-016-4229-7. Ikon N, & Ryan RO. (2017) Barth syndrome: connecting cardiolipin to cardiomyopathy. Lipids. 1-10

Adapted, with permission, from DOI: 10.1016/j.bbrc.2015.07.012. Ikon N, Su B, Hsu FF, Forte TM, Ryan RO. (2015) Exogenous cardiolipin localizes to mitochondria and prevents TAZ knockdown-induced apoptosis in myeloid progenitor cells. Biochemical and Biophysical Research Communications. 128(2), 442–457.

Chapter 1: Barth Syndrome: Connecting Cardiolipin to Cardiomyopathy

Introduction

Barth Syndrome (BTHS) is a rare X-linked recessive disorder characterized by cardiolipin abnormalities, lactic acidosis, organic aciduria, skeletal muscle weakness, neutropenia, and cardiomyopathy [1]. The underlying cause of BTHS has been definitively traced to mutations in the *TAZ* gene [2, 3]. This discovery launched a concerted research effort to decipher how mutations in *TAZ* lead to the BTHS phenotype. A key finding revealed that *TAZ* encodes a phospholipid transacylase, termed tafazzin [4, 5]. Defective tafazzin activity leads to alterations in the content and composition of cardiolipin and the appearance of monolysocardiolipin [6]. Experimental models of BTHS, including yeast [7], *Drosophila* [8], zebrafish [9] and mice [10] have validated a cause / effect relationship between *TAZ* mutations and cardiolipin abnormalities. Evidence of the impact of changes in cardiolipin content and composition can be seen by morphological changes to the inner mitochondrial membrane (IMM) associated with BTHS [11]. This chapter describes how mutations in *TAZ*, through their effects on mitochondrial function, manifest as organic aciduria, skeletal muscle weakness, and cardiomyopathy.

TAZ mutations and cardiolipin remodeling.

The tafazzin transacylase localizes to mitochondria and functions in remodeling cardiolipin fatty acyl chains. Cardiolipin is distinct from other glycerophospholipids in that two phosphatidate moieties share the same glycerol head group. This gives rise to an anionic phospholipid with four esterified fatty acyl chains and a cone-shaped structure. In eukaryotes, cardiolipin is mainly confined to the IMM [12]. Interestingly, unlike most tissues, up to 90% of cardiolipin in cardiac and skeletal muscle mitochondria exists as a single molecular species, tetralinoleoylcardiolipin [12]. Establishment and maintenance of this molecular species composition depends on phospholipid remodeling reactions that involve tafazzin transacylase activity [13]. An *in vitro* transacylation reaction catalyzed by tafazzin is shown in **Figure 1**. Acyl chain transfer from the sn-2 position of phosphatidylcholine to the corresponding hydroxyl of monolysocardiolipin is depicted. Although phosphatidylcholine is the acyl chain donor in this image, phospholipids with other head groups can also serve as acyl group donor in this reaction [14,15]. In addition to tafazzin-mediated transacylation, cardiolipin remodeling can occur via the endoplasmic reticulum (ER) localized enzyme, acyl CoA lysocardiolipin acyltransferase (ALCAT1). In this reaction a fatty acid from fatty acyl CoA is transferred to monolysocardiolipin to produce cardiolipin [15,16]. In addition to ALCAT1, a mitochondrial monolysocardiolipin acyltransferase (MLCAT) has been reported that catalyzes acylation of monolysocardiolipin in a reaction that employs linoleoyl-CoA as substrate [17,18]. Whereas the relative contributions of these alternate routes to the pool of mature cardiolipin in the IMM are unclear at present, the fact that *TAZ* mutations correlate with characteristic changes in cardiolipin content and composition indicates ALCAT1- and MLCAT-mediated reactions are not able to fully compensate for loss of tafazzin.

Individuals harboring mutations in *TAZ* (i.e. BTHS) manifest compromised or missing tafazzin enzymatic activity. This results in specific alterations in cardiolipin, including increased molecular species heterogeneity, decreased levels of cardiolipin, and increased levels of monolysocardiolipin [6]. If a given *TAZ* mutation gives rise to a tafazzin

protein with residual enzyme activity, lesser changes in cardiolipin content and composition, and a milder phenotype, may be anticipated [19]. Conversely, more severe mutations in *TAZ* that lead to complete loss of transacylase activity, will have a more deleterious effect in terms of both IMM structure and the function of proteins embedded therein. Despite this, *TAZ* mutations have been described [20] in which the correlation between genotype and phenotype is not apparent. Conceivably, individual differences in *TAZ* mRNA splicing, mRNA stability, or differences in tafazzin protein turnover rate could affect residual enzyme activity. By the same token, one or more extraneous phenotypic modifiers, ranging from environmental to biochemical, could be responsible for differences in the degree of disease manifestation.

Altered cardiolipin composition affects the electron transport chain

Insofar as electron transport chain (ETC) proteins are embedded in the IMM, it is not surprising that alterations in the phospholipid component of this membrane have a measurable impact on aerobic metabolism [21]. Indeed, the effect of perturbations in IMM lipid content and/or composition on the functional properties of ETC proteins are likely amplified by the fact that the IMM is one of the most protein-rich membranes in nature. Unlike an average bilayer membrane, which contains 30 - 50 % protein, the IMM is comprised of ~75 % protein and 25 % lipid by mass. Given this exceptionally high protein content, changes in its phospholipid composition are likely to impact the structure, orientation and/or activity of IMM proteins. Indeed, studies have shown that cardiolipin directly interacts with each of the five protein complexes that comprise the ETC [12, 22, 23]. Moreover, cardiolipin is required for the optimal function of complexes I, III, and IV, and this function is not retained when cardiolipin is substituted by other phospholipids, including monolysocardiolipin [22, 24, 25]. Consistent with its altered cardiolipin content, the activity of ETC proteins is decreased in BTHS [26, 27]. In addition to direct interaction with proteins of the ETC, cardiolipin also serves a structural role in the IMM, including maintenance of membrane integrity. Perturbations that compromise IMM integrity would be anticipated to result in dissipation of the proton gradient that drives ADP phosphorylation. In keeping with this, BTHS mitochondria exhibit a decreased membrane potential, a decreased respiratory coupling index, and increased proton leak [28-30]. Leakage of protons across the IMM can also lead to formation of free radicals and increased levels of reactive oxygen species which, in turn, exacerbate mitochondrial impairment [29, 30].

It is noteworthy that the IMM contains numerous folds and invaginations, termed cristae. Due to its distinctive cone-shaped structure, cardiolipin segregates to regions of negative membrane curvature [31, 32]. In BTHS, defective cardiolipin remodeling correlates with profound changes in cristae ultrastructure [11, 33, 34]. Furthermore, cardiolipin contributes to the stability of ETC supercomplexes, thereby promoting efficient electron transfer between individual complexes of the ETC [35, 36]. BTHS mitochondria have reduced levels of supercomplexes and display decreased stability of existing supercomplexes [30, 37]. Similarly, Huang et al [38] reported that ETC supercomplexes are destabilized in cardiolipin-depleted mitochondria from *taz* knockdown mouse hearts, a condition that presumably has an adverse effect on metabolic channeling of reducing

equivalents. Likewise, Kiebish et al [39] reported that loss of tafazzin function in myocardium leads to changes in the mitochondrial lipidome, resulting in the dysregulated generation of oxidized derivatives of polyunsaturated fatty acids. A generalized model depicting the impact of cardiolipin impairment in BTHS on ETC activity is summarized in **Figure 2**. The net effect of this impairment is a decreased ability to generate ATP through oxidation of the respiratory intermediates, NADH and $FADH_2$.

NADH / $FADH_2$ accumulation inhibits TCA cycle enzymes

For each acetyl CoA oxidized via the TCA cycle, three NADH and one $FADH_2$ are generated. As NADH and $FADH_2$ are oxidized back to NAD^+ and FAD^+, respectively, electrons funnel into the ETC. Their passage from low to high standard reduction potential supports establishment of a proton gradient across the IMM that functions as the driving force for F_1 ATPase-mediated phosphorylation of ADP. In a working muscle, this sequence of events is constantly repeated, providing muscle fibers with a steady supply of ATP. At rest, less ATP is required and, correspondingly, less fuel consumption occurs. Muscle has a limited capacity to store the energy of ATP (e.g. phosphocreatine) such that, when muscle activity increases, metabolic activity necessary to generate ATP also increases. In a normal mitochondrion, oxidation of NADH and $FADH_2$ is highly efficient. High NADH ubiquinone oxidoreductase (Complex I) activity maintains NADH levels at very low levels [40]. Maintenance of this disproportionate ratio requires efficient movement of electrons from Complex I to Complex III (Coenzyme Q – cytochrome c reductase) and is essential for proper functioning of mitochondrial enzymes that employ NAD^+ as substrate (e.g. isocitrate dehydrogenase, α-ketoglutarate dehydrogenase, malate dehydrogenase and others). If NADH levels rise in the matrix, product inhibition of these enzymes will occur (**Figure 3**) [41, 42]. In BTHS, *TAZ* mutation-induced alterations in cardiolipin impair ETC function, decreasing the rate of electron transfer reactions. When this occurs, oxidation of NADH does not keep pace with its production and the ratio of NAD^+ / NADH decreases [30]. As the concentration of NADH rises, product inhibition of TCA cycle enzymes that employ NAD^+ as a substrate occurs.

Inefficient respiration drives anaerobic glucose metabolism / lactic acidosis

Demand for ATP by cardiac tissue is persistent. Even at rest, cardiac muscle contraction requires a continuous supply of ATP. Furthermore, any activity that accelerates the heart rate will increase demand for ATP. Normally, oxidative phosphorylation is the principal means by which ATP is generated and, as such, cardiac tissue contains abundant mitochondria that align adjacent to muscle fibers. As contractile activity increases, aerobic respiration and metabolic fuel consumption follow suit. In BTHS, however, a bottleneck occurs because alterations in cardiolipin content and composition that affect the IMM lead to ETC inefficiency, a decreased rate of NADH and $FADH_2$ oxidation, and subsequent inhibition of TCA cycle enzymes. The resulting slowdown in ATP production reaches a point wherein aerobic respiration fails to meet the energy demands of the tissue. Because survival depends on sustained cardiac muscle contraction, the tissue adapts by increasing anaerobic glycolysis and activating the Cori cycle (**Figure 4**) [21]. Under

normal circumstances, pyruvate dehydrogenase converts pyruvate to acetyl CoA that enters the TCA cycle and is metabolized to CO_2. However, during anaerobic conditions, pyruvate is instead converted to lactate by lactate dehydrogenase. Lactate, thus formed, exits the cell and migrates to liver where it is converted to glucose via gluconeogenesis. Once formed, this glucose is secreted from hepatocytes and returns to muscle / heart where anaerobic glycolysis starts the cycle anew. Reliance on the Cori cycle to generate ATP for cardiac muscle contraction is problematic, however. As glucose utilization increases, lactic acid buildup leads to a decrease in blood pH (i.e. lactic acidosis). Furthermore, the entire process operates at an energy deficit since 6 ATP are required to generate glucose from lactate via gluconeogenesis in liver while anaerobic metabolism of glucose to lactate in muscle yields 2 ATP. Thus, although this process provides a stopgap means to generate ATP when oxidative metabolism is limiting, its meager ATP yield, buildup of lactic acid and increased demand for gluconeogenesis will lead to problems over time. Consistent with this, subjects with BTHS manifest lactic acidosis, skeletal muscle weakness, lethargy and cardiomyopathy [1, 43].

TCA cycle inhibition results in metabolite diversion into organic acids

As NADH and $FADH_2$ levels rise in the matrix of skeletal muscle and cardiac tissue mitochondria, collateral metabolic repercussions occur. In these tissues, as TCA cycle activity slows, acetyl CoA and propionyl CoA accumulate. Above a threshold acetyl CoA concentration, the enzyme T2 thiolase reverses direction and catalyzes condensation of 2 acetyl CoA, forming acetoacetyl CoA plus CoASH. Acetoacetyl CoA subsequently reacts with another acetyl CoA to form 3-hydroxy 3-methylglutaryl CoA (HMG CoA) via HMG CoA synthase 2. Under the prevailing metabolic conditions in BTHS mitochondria, HMG CoA is diverted to 3-methylglutaconyl CoA (3MG CoA) via 3MG CoA hydratase, a leucine degradation pathway enzyme that normally functions in the reverse direction [45, 46]. As levels of 3MG CoA rise, this metabolite becomes a substrate for acyl CoA thioesterase-mediated hydrolysis, producing the dead end organic acid, 3-methylglutaconic acid (3MGA), that is abundant in urine of BTHS subjects but essentially absent in normal subjects (**Figure 5**). In addition to 3MGA, a portion of the 3MG CoA pool is reduced to 3-methylglutaryl CoA followed by thioester hydrolysis to yield a second organic acid, 3-methylglutaric acid. At present the identity of the oxidoreductase responsible for conversion of 3MG CoA to 3-methylglutaryl CoA or the thioesterase that generates the product, 3-methylglutarate, are unknown. It is presumed, however, that 3MG CoA and 3-methyglutaryl CoA serve as alternate substrates for the enzyme(s) involved.

Whereas 3MGA and 3-methylglutarate are derived from acetyl CoA, elevated levels of propionyl CoA are largely responsible for formation of a third, less abundant organic acid. Despite some progress, the identity of this organic acid is not yet clear. In 1991, Kelley et al [43] reported the presence of 2-ethylhydracrylic acid (2-EHA) in urine of BTHS subjects. A relatively rare organic acid, 2-EHA is proposed to arise from an obscure alternate pathway of isoleucine metabolism [47, 48]. Insofar as no isoleucine metabolism pathway defects have been reported in BTHS, the molecular basis for production of 2-EHA is not readily apparent. Of interest, however, is the fact that T2

thiolase not only functions as the terminal enzyme in ß-oxidation, it also catalyzes the final step of isoleucine degradation, cleaving 2-methylacetoacetyl CoA into propionyl CoA plus acetyl CoA. As propionyl CoA levels rise in the presence of acetyl CoA, T2 thiolase reverses direction and catalyzes a more complex set of reactions [49]. Condensation of acetyl CoA and propionyl CoA can generate the isoleucine degradation pathway intermediate, 2-methylacetoacetyl CoA and buildup of this metabolite (or 3-hydroxy, 2-methylbutyryl CoA) could interfere with isoleucine-derived metabolite flux. When this occurs, proximal intermediates in the isoleucine degradation pathway can undergo enol-keto tautomerization, converting (*S*) enantiomers to the corresponding (*R*) intermediates that, subsequently, are metabolized by 3 valine metabolic pathway enzymes as alternate substrates, leading to formation of 2-EHA [50]. By the same token, if propionyl CoA loads onto T2 thiolase before acetyl CoA, the expected condensation product is n-3-ketovaleryl CoA. Under the prevailing metabolic conditions in BTHS, NADH dependent dehydrogenation will generate n-3-hydroxyvaleryl CoA and subsequent thioester hydrolysis will generate n-3-hydroxyvaleric acid, an organic acid previously observed in propionyl CoA carboxylase deficiency and methylmalonyl CoA mutase deficiency [51-53]. Insofar as the molecular mass of 2-EHA and n-3-hydroxyvalerate are identical (118 Da), careful organic acid analysis will be necessary to distinguish their relative contributions to the profile observed in urine of BTHS subjects.

Insufficient ATP production initiates cellular / tissue damage leading to dilated cardiomyopathy

When cardiac muscle is unable to contract efficiently, over time, tissue damage occurs that is manifest as cardiomyopathy. Characteristic cardiac abnormalities associated with BTHS normally present in the first year of life, usually as dilated cardiomyopathy or left ventricular non-compaction (LVNC) [21]. LVNC is a distinct cardiomyopathy characterized by trabeculations and intertrabecular recesses in the ventricular myocardium, which are caused by disruption of the endocardium and myocardium during embryogenesis.. The fact that these anatomical defects, as well as disorders of mitochondrial energy metabolism, both lead to LVNC suggests this condition can arise from different origins [57]. Hemodynamic analysis of BTHS subjects normally reveals a reduced ejection fraction and increased left ventricular internal dimension in diastole [26, 58]. The link between mitochondrial cardiolipin defects and these morphologic / functional myocardial features are poorly understood. Notwithstanding the possible contribution of cardiomyocyte apoptosis, it is likely that an inability to sustain muscle contraction, owing to a limiting supply of ATP, underlies the phenotype [59]. Moreover, the observation that mutations in *TAZ* can lead to LVNC is in keeping with various metabolic effects described above and points to a direct connection between compromised energy metabolism and cardiomyopathy.

A contracted muscle is up to one third shorter than its extended length due to decrease length of sarcomeres. The basic unit of striated muscle, sarcomeres are comprised of long fibrous proteins organized as filaments that slide past each other during contraction and relaxation. The mechanics of the process, which involves interaction between myosin and actin, is driven by ATP hydrolysis. Under low ATP conditions ,

myosin does not bind actin and fails to undergo the conformational change that pulls against actin (i.e. the power stroke). When sufficient quantities of ATP are not available, sarcomeres cannot contract uniformly. When this occurs, the tissue weakens and ejection volumes decrease. Left ventricle filling, followed by a partial or incomplete contractile event, increases chamber volume, stretches the tissue and promotes thinning of the ventricle wall (i.e. dilation). Support for this general concept is seen by distinctive mutations in myosin. Interestingly, mutations that increase the myosin power stroke above normal lead to hypertrophic cardiomyopathy while others that decrease the power stroke result in dilated cardiomyopathy. For example, Phe764Leu or Ser532Pro mutations in myosin correlate with diminished power production and are associated with dilated cardiomyopathy [60]. Analogous to these myosin mutations that directly affect contractility, mutations in *TAZ* elicit a similar, albeit indirect, effect by compromising the ability of mitochondria to generate ATP. Whereas the left ventricle is the first tissue site to exhibit pathology, as damage spreads to the right ventricle and atria, the disease worsens. As the heart chambers dilate, contractility declines further and blood circulation decreases, exacerbating the physiological impairment. In the absence of intervention, the heart will continue to weaken and, ultimately, fail.

In normal subjects, cardiomyocytes respond to an increase in heart rate by increasing production of ATP via aerobic metabolism. Whereas BTHS cardiac tissue may be able to satisfy tissue needs for ATP under resting conditions, it is unable to adequately ramp up production to meet an increase in demand [21]. An interesting question relates to why cardiac crises often present at key life stage junctions including the first few months of life, 2-4 years of age and puberty. One possibility is that these crises are precipitated by the rapid growth characteristic of these stages of development [63]. As the heart already has one of the highest metabolic rates of any organ [64], the increased energy required for tissue growth is expected to put extra strain on cardiac tissue such that damage / failure is more likely to occur. An inability to increase aerobic respiration in response to physiological need is also directly responsible for two hallmark phenotypic features of BTHS, lactic acidosis and organic aciduria. Thus, their presence is a telltale sign that the tissue is laboring to meet the physiological demand for ATP and, unless this demand is reduced, tissue damage (i.e. cardiomyopathy) will result.

BTHS is not the only disease that causes decreased cardiolipin content, alterations in acyl chain composition, and lipid peroxidation. These symptoms are associated with mitochondrial dysfunction in pathological conditions ranging from ischemia to hypothyroidism to heart failure and aging [54]. In particular, age-related heart failure is associated with decreased levels of tetralinoleoylcardiolipin and myocardial dysfunction [18, 55]. The aged heart exhibits impaired metabolic efficiency, a decreased capacity to oxidize fatty acids and enhanced dependence on glucose metabolism. Furthermore, aging impairs mitochondrial oxidative phosphorylation due to a decrease in the activity of complexes III and IV [56]. Thus, although BTHS is a rare disorder, it shares features with major chronic diseases and aging-related processes. Insofar as BTHS it is caused by a single gene defect, studies of this disorder provide a unique opportunity to obtain insight into the mechanism whereby a defective cardiolipin profile leads to cardiac dysfunction.

Concluding Remarks

In this chapter, we have navigated the circuitous path from mutations in *TAZ*, a gene encoding a phospholipid transacylase, to manifestation of cardiomyopathy. The presence of key phenotypic features, including alterations in the content and composition of cardiolipin, lactic acidosis, organic aciduria, and muscle fatigue, fit into a model of defective mitochondrial ATP production that leads to an energy deficit. In turn, lack of sufficient ATP limits muscle contractility and underlies cellular and tissue damage that manifests as dilated cardiomyopathy and LVNC. The remarkable finding that mutations in a seemingly innocuous phospholipid transacylase have such a profound impact on cardiac/skeletal muscle metabolism and contractile function reveals a set of tightly interconnected processes that underpin efficient muscle physiology and metabolism. Moreover, although BTHS subjects can function “normally” at rest, when stressed (e.g. sustained increase in heart rate) disease manifests by failure to generate sufficient quantities of ATP. When this occurs, compensatory metabolic and cell biological changes occur that lead to tissue damage. To assess whether improved fitness may improve outcomes, or be curative, for BTHS, Cade et al [61] investigated whether endurance exercise training improves exercise tolerance by measuring skeletal muscle oxygen extraction, cardiac function, and quality of life in young adults with BTHS. Whereas twelve weeks of endurance exercise training was found to be safe, only minor improvements in peak exercise tolerance were recorded, and training did not appear to improve skeletal muscle oxygen extraction or cardiac function. However, while exercise may not be the best means of combatting BTHS-related symptoms, interventions aimed at improving mitochondrial function and energy balance will likely be the key to managing this disease. The most intriguing possibility in this line of inquiry is the potential to restore mitochondrial function without the need for a functional tafazzin. It has been shown that linoleic acid supplementation of cultured BTHS fibroblasts resulted in an increase in tetralinoleoyl CL [64], suggesting that a deficiency in tafazzin-mediated CL remodeling can be bypassed. The amounts of linoleic acid required make this approach unfeasible in human subjects, but if tetralinoleoyl CL could be solubilized and delivered to cells directly, it could open the door for the first direct treatment of BTHS.

Figures

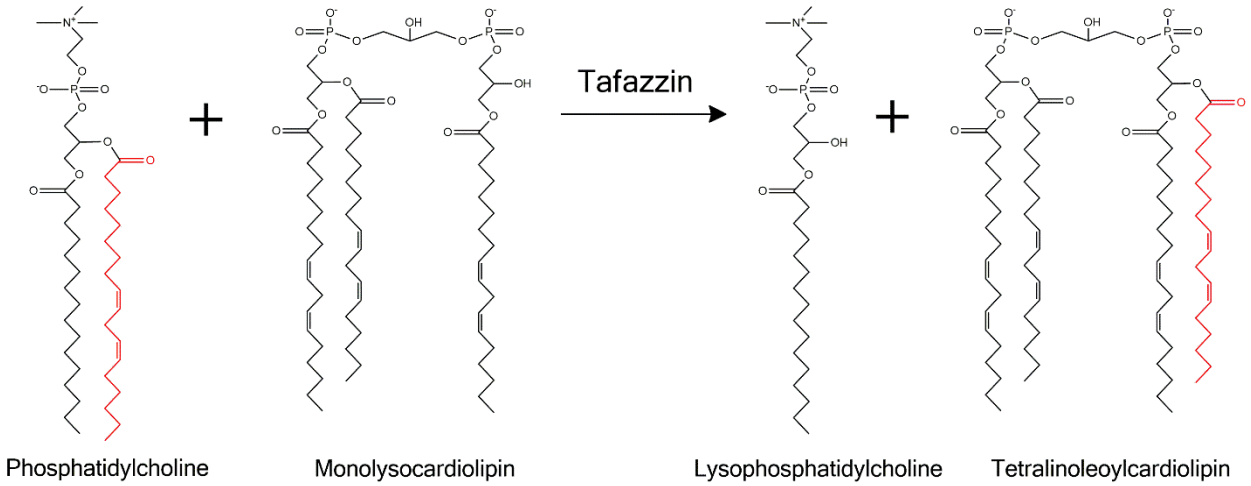

Figure 1. **Tafazzin-mediated transacylation activity**. The tafazzin enzyme has been shown to catalyze transfer of an acyl group (red) from phospatidylcholine (or other phospholipids) to monolysocardiolipin. Through an iterative process that may involve additional enzymatic reactions, tafazzin functions in maturation of nascent cardiac and skeletal muscle cardiolipin, resulting in a predominantly uniform molecular species, tetralinoleoylcardiolipin.

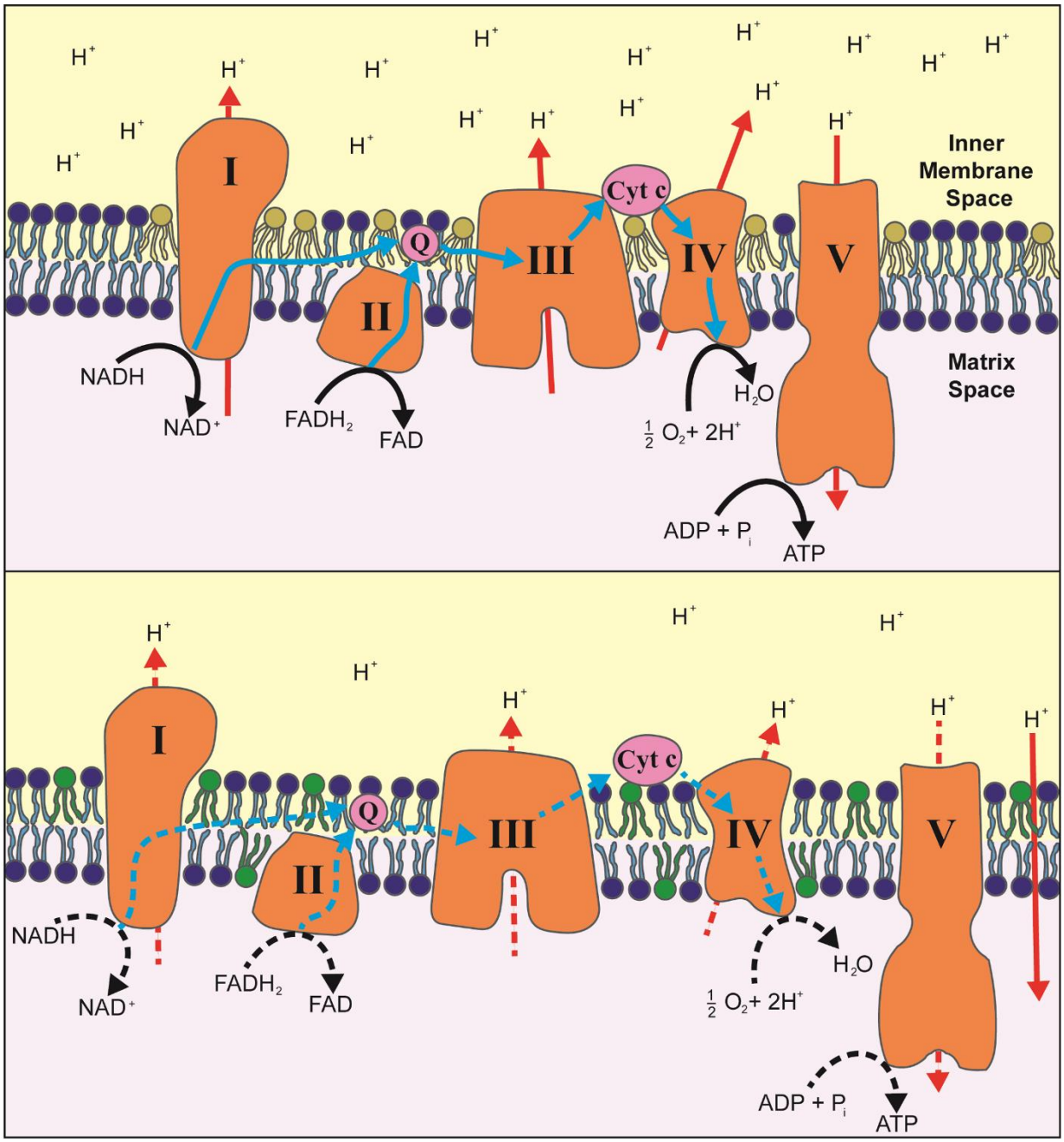

Figure 2. **Efficient ETC activity is required for sustained aerobic ATP production**. Two key products of fuel metabolism in the matrix, NADH and $FADH_2$, are oxidized to NAD^+ and FAD^+ by Complex I and II of the ETC, respectively. The flow of electrons to Complexes III and IV via coenzyme Q and cytochrome c, respectively, is coupled to proton movement to the inner membrane space (Upper panel). The proton gradient thus formed drives oxidative phosphorylation via Complex V (F_1 ATPase). When the content and composition of cardiolipin in the IMM is perturbed by *TAZ* mutations (Lower panel) the orientation, stability and function of ETC complexes are affected in a manner that compromises electron flow (dashed lines). Likewise decreased membrane integrity can increase proton leakage (solid red line).

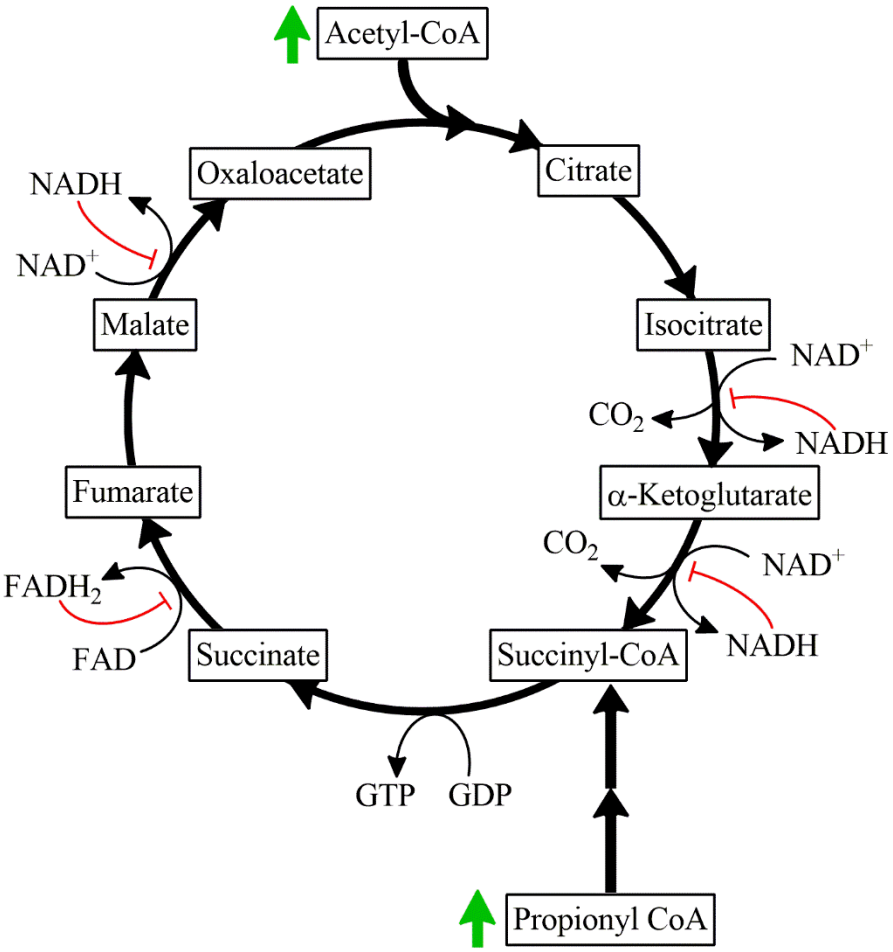

Figure 3. **Effect of NADH / $FADH_2$ accumulation on TCA cycle activity**. When *TAZ* mutation-dependent alterations in cardiolipin content and composition interfere with ETC activity, NADH and $FADH_2$ accumulate in the matrix space. Elevated levels of the reduced form of these coenzymes lead to product inhibition of TCA cycle enzymes, slowing / shutting down the cycle. Unable to enter the TCA cycle, acetyl CoA and propionyl CoA accumulate in the matrix space of skeletal muscle and cardiac tissue mitochondria.

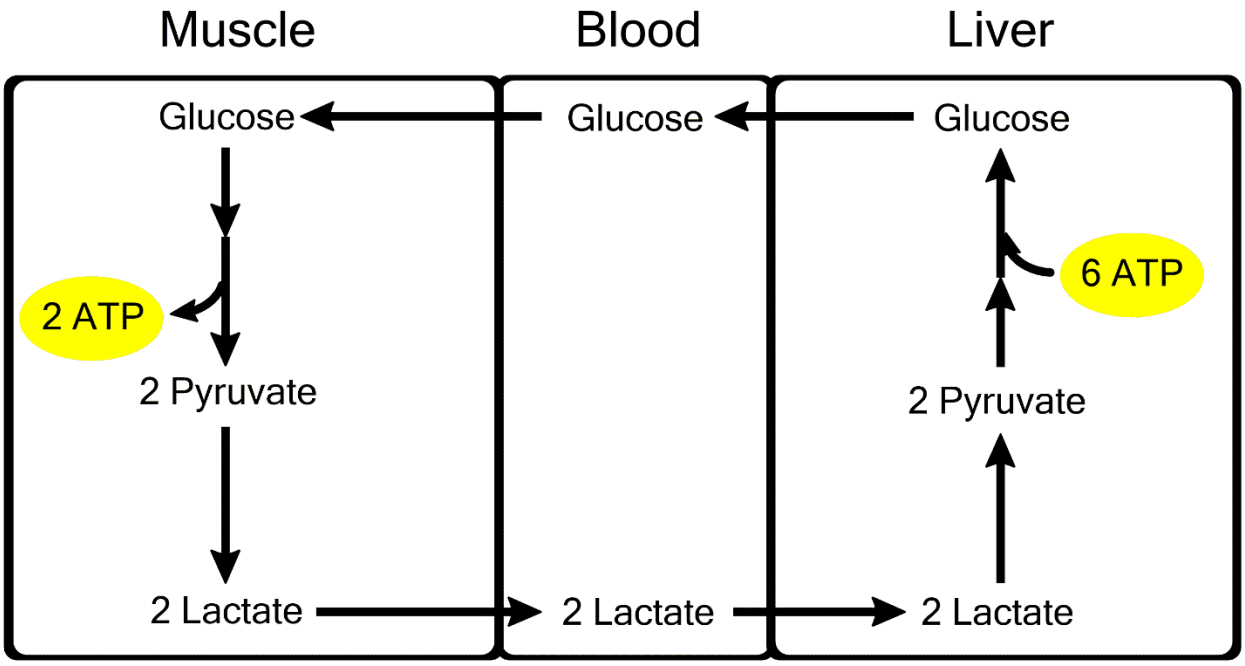

Figure 4. **Inhibition of oxidative metabolism induces Cori cycle activity**. As TCA cycle activity slows in cardiac and skeletal muscle tissue due to compromised ETC function and buildup of NADH and $FADH_2$, a shift in metabolism occurs wherein anaerobic metabolism increases and the pyruvate generated is converted to lactate. Lactate migrates to liver where gluconeogenesis converts lactate to glucose, at the expense of 6 ATP. Glucose generated in hepatocytes via this process transits back to muscle where glycolysis yields 2 ATP for use in muscle contraction.

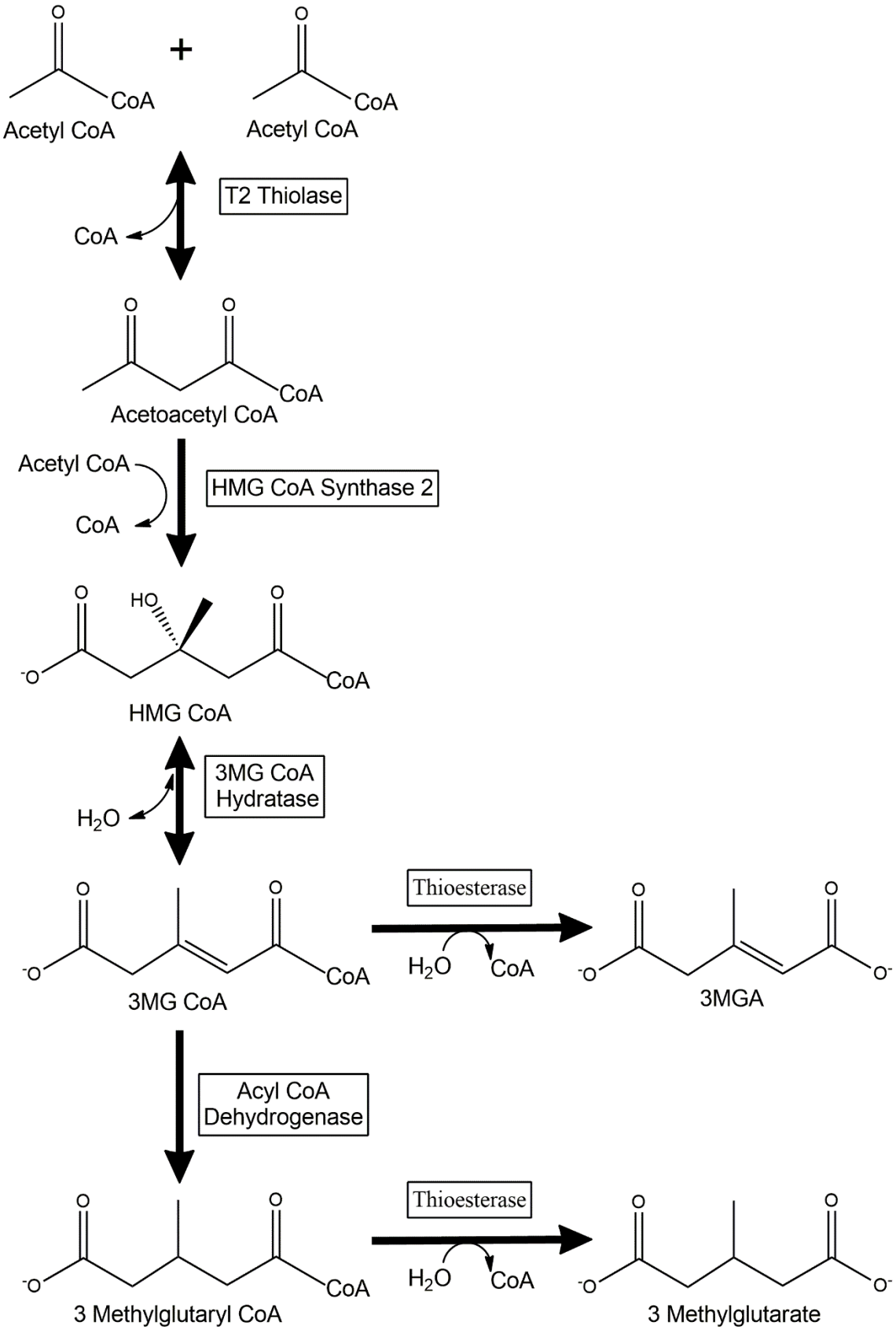
Acetyl CoA
Acetyl CoA
T2 Thiolase
CoA
Acetoacetyl CoA
Acetyl CoA
CoA
HMG CoA Synthase 2
HO
HMG CoA
3MG CoA Hydratase
H2O
3MG CoA
Thioesterase
H2O
CoA
3MGA
Acyl CoA Dehydrogenase
3 Methylglutaryl CoA
Thioesterase
H2O
CoA
3 Methylglutarate

Figure 5. **Diversion of acetyl CoA to organic acid waste products**. The inability to oxidize acetyl CoA via the TCA cycle leads to transient accumulation of this metabolite. Above a threshold concentration the enzyme T2 thiolase reverses direction and condenses 2 acetyl CoA into acetoacetyl CoA plus CoASH. Further condensation of acetoacetyl CoA and acetyl CoA generates HMG CoA that is converted to 3-methylglutaconyl CoA (3MG CoA) by 3MG CoA hydratase. As the concentration of 3MG CoA increases it becomes a substrate for thioesterase-mediated hydrolysis (forming 3-methylglutaconic acid; 3MGA) or oxidoreductase-mediated conversion to 3-methylglutaryl CoA. This latter metabolite is subsequently hydrolyzed to 3-methylglutarate and excreted in urine along with 3MGA.

References

[1] Clarke SL, Bowron A, Gonzalez IL, Groves SJ, Newbury-Ecob R, Clayton N, Martin RP, Tsai-Goodman B, Garratt V, Ashworth M, Bowen VM, McCurdy KR, Damin MK, Spencer CT, Toth MJ, Kelley RI, Steward CG (2013) Barth syndrome. Orphanet J Rare Dis 8:23

[2] Bione S, D'Adamo P, Maestrini E, Gedeon AK, Bolhuis PA, Toniolo D (1996) A novel X-linked gene, G4.5. is responsible for Barth syndrome. Nat Genet 12:385-389

[3] Whited K, Baile MG, Currier P, Claypool SM (2013) Seven functional classes of Barth syndrome mutation. Hum Mol Genet 22:483-492

[4] Xu Y, Kelley RI, Blanck TJ, Schlame M (2003) Remodeling of cardiolipin by phospholipid transacylation. J Biol Chem 278:51380-51385

[5] Xu Y, Malhotra A, Ren M, Schlame M (2006) The enzymatic function of tafazzin. J Biol Chem 281:39217-39224

[6] Valianpour F, Mitsakos V, Schlemmer D, Towbin JA, Taylor JM, Ekert PG, Thorburn DR, Munnich A, Wanders RJ, Barth PG, Vaz FM (2005) Monolysocardiolipins accumulate in Barth syndrome but do not lead to enhanced apoptosis. J Lipid Res 46:1182-1195

[7] Gu Z, Valianpour F, Chen S, Vaz FM, Hakkaart GA, Wanders RJ, Greenberg ML (2004) Aberrant cardiolipin metabolism in the yeast taz1 mutant: a model for Barth syndrome. Mol Microbiol 51:149-158

[8] Xu Y, Condell M, Plesken H, Edelman-Novemsky I, Ma J, Ren M, Schlame M (2006a) A Drosophila model of Barth syndrome. Proc Natl Acad Sci USA 103:11584-11588

[9] Khuchua Z, Yue Z, Batts L, Strauss AW (2006) A zebrafish model of human Barth syndrome reveals the essential role of tafazzin in cardiac development and function. Circ Res 99:201-208

[10] Acehan D, Vaz F, Houtkooper RH, James J, Moore V, Tokunaga C, Kulik W, Wansapura J, Toth MJ, Strauss A, Khuchua Z (2011) Cardiac and skeletal muscle defects in a mouse model of human Barth syndrome. J Biol Chem 286:899-908

[11] Acehan D, Khuchua Z, Houtkooper RH, Malhotra A, Kaufman J, Vaz FM, Ren M, Rockman HA, Stokes DL, Schlame M (2009) Distinct effects of tafazzin deletion in differentiated and undifferentiated mitochondria. Mitochondrion 9:86-95

[12] Houtkooper RH, Vaz FM (2008) Cardiolipin, the heart of mitochondrial metabolism. Cell Mol Life Sci 65:2493-2506

[13] Schlame M (2009) Formation of molecular species of mitochondrial cardiolipin 2. A mathematical model of pattern formation by phospholipid transacylation. Biochim Biophys Acta 1791:321-325

[14] Malhotra A, Xu Y, Ren M, Schlame M (2009) Formation of molecular species of mitochondrial cardiolipin. 1. A novel transacylation mechanism to shuttle fatty acids between sn-1 and sn-2 positions of multiple phospholipid species. Biochim Biophys Acta 1791:314-320

[15] Gaspard GJ, McMaster CR (2015) Cardiolipin metabolism and its causal role in the etiology of the inherited cardiomyopathy Barth syndrome. Chem Phys Lipids 193:1-10

[16] Cao J, Liu Y, Lockwood J, Burn P, Shi Y (2004) A novel cardiolipin-remodeling pathway revealed by a gene encoding an endoplasmic reticulum-associated acyl-CoA:lysocardiolipin acyltransferase (ALCAT1) in mouse. J Biol Chem. 279:31727-31734

[17] Taylor WA, Hatch GM (2009) Identification of the human mitochondrial linoleoyl-coenzyme A monolysocardiolipin acyltransferase (MLCL AT-1). J Biol Chem. 284: 30360-30371

[18] Mejia EM, Cole LK, Hatch GM (2014) Cardiolipin metabolism and the role it plays in heart failure and mitochondrial supercomplex formation. Cardiovasc Hematol Disord Drug Targets 14:98-106

[19] Ye C, Shen Z, Greenberg ML (2016) Cardiolipin remodeling: a regulatory hub for modulating cardiolipin metabolism and function. J Bioenerg Biomembr 48:113-123

[20] Ronvelia D, Greenwood J, Platt J, Hakim S, Zaragoza MV (2012) Intrafamilial variability for novel TAZ gene mutation: Barth syndrome with dilated cardiomyopathy and heart failure in an infant and left ventricular noncompaction in his great-uncle. Mol Genet Metab 107:428-32

[21] Spencer CT, Byrne BJ, Bryant RM, Margossian R, Maisenbacher M, Breitenger P, Benni PB, Redfearn S, Marcus E, Cade WT (2011) Impaired cardiac reserve and severely diminished skeletal muscle O(2) utilization mediate exercise intolerance in Barth syndrome. Am J Physiol Heart Circ Physiol 301:H2122-2129

[22] Fry M, Green, DE (1981) Cardiolipin requirement for electron transfer in complex I and III of the mitochondrial respiratory chain. J Biol Chem 256:1874-1880

[23] Eble KS, Coleman WB, Hantgan RR, Cunningham CC (1990) Tightly associated cardiolipin in the bovine heart mitochondrial ATP synthase as analyzed by 31P nuclear magnetic resonance spectroscopy. J Biol Chem 265:19434-19440

[24] Robinson NC, Zborowski J, Talbert L H (1990) Cardiolipin-depleted bovine heart cytochrome c oxidase: binding stoichiometry and affinity for cardiolipin derivatives. Biochemistry 29:8962-8969

[25] Hoffmann B, Stöckl A, Schlame M, Beyer K, Klingenberg M (1994). The reconstituted ADP/ATP carrier activity has an absolute requirement for cardiolipin as shown in cysteine mutants. J Biol Chem 269:1940-1944

[26] Christodoulou J, McInnes RR, Jay V, Wilson G, Becker LE, Lehotay DC, Platt BA, Bridge PJ, Robinson BH, Clarke JT (1994) Barth syndrome - clinical observations and genetic-linkage studies. Amer J Med Gen 50:255–264

[27] Barth PG, Van Den Bogert C, Bolhuis PA, Scholte HR, van Gennip AH, Schutgens RB, Ketel AG (1996) X-linked cardioskeletal myopathy and neutropenia (Barth syndrome): Respiratory-chain abnormalities in cultured fibroblasts. J Inherit Metabol Dis 19:157–160

[28] Xu Y, Sutachan JJ, Plesken H, Kelley RI, Schlame M (2005) Characterization of lymphoblast mitochondria from patients with Barth syndrome. Lab Invest 85:823–830

[29] Wang G, McCain ML, Yang L He A, Pasqualini FS, Agarwal A, Yuan H, Jiang D, Zhang D, Zangi L, Geva J, Roberts AE, Ma Q, Ding J, Chen J, Wang DZ, Li K, Wang J, Wanders RJ, Kulik W, Vaz FM, Laflamme MA, Murry CE, Chien KR, Kelley RI, Church GM, Parker KK, Pu WT (2014) Modeling the mitochondrial cardiomyopathy of Barth syndrome with induced pluripotent stem cell and heart-on-chip technologies. Nature Med 20:616–623

[30] Gonzalvez F, D'Aurelio M, Boutant M, Moustapha A, Puech JP, Landes T, Arnauné-Pelloquin L, Vial G, Taleux N, Slomianny C, Wanders RJ, Houtkooper RH, Bellenguer P, Møller IM, Gottlieb E, Vaz FM, Manfredi G, Petit PX (2013) Barth syndrome: Cellular compensation of mitochondrial dysfunction and apoptosis inhibition due to changes in cardiolipin remodeling linked to tafazzin (TAZ) gene mutation. Biochim Biophys Acta 1832:1194–1206

[31] Schlame M, Acehan D, Berno B, Xu Y, Valvo S, Ren M, Stokes DL, Epand RM (2012) The physical state of lipid substrates provides transacylation specificity for tafazzin. Nat Chem Biol 8:862–869

[32] Renner LD, Weibel DB (2011) Cardiolipin microdomains localize to negatively curved regions of Escherichia coli membranes. Proc Natl Acad Sci USA 108:6264-6269

[33] Bissler JJ, Tsorads M, Goring HH, Hug P, Chuck G, Tombragel E, McGraw C, Schlotman J, Ralston MA, Hug G (2002) Infantile dilated X-linked cardiomyopathy, G4. 5 mutations, altered lipids, and ultrastructural malformations of mitochondria in heart, liver, and skeletal muscle. Lab Invest 82:335-344

[34. Acehan D, Xu Y, Stokes DL, Schlame M (2007) Comparison of lymphoblast mitochondria from normal subjects and patients with Barth syndrome using electron microscopic tomography. Lab Invest 87:40–48

[35] Zhang M, Mileykovskaya E, Dowhan W (2005) Cardiolipin is essential for organization of complexes III and IV into a supercomplex in intact yeast mitochondria. J Biol Chem 280:29403-29408

[36] Bazan S, Mileykovskaya E, Mallampalli VK, Heacock P, Sparagna GC, Dowhan W (2013) Cardiolipin-dependent reconstitution of respiratory supercomplexes from purified Saccharomyces cerevisiae complexes III and IV. J Biol Chem 288:401-411

[37] McKenzie M, Lazarou M, Thorburn DR, Ryan, MT (2006) Mitochondrial respiratory chain supercomplexes are destabilized in Barth Syndrome patients. J Mol Biol 361:462-469

[38] Huang Y, Powers C, Madala SK, Greis KD, Haffey WD, Towbin JA, Purevjav E, Javadov S, Strauss AW, Khuchua Z (2015) Cardiac metabolic pathways affected in the mouse model of barth syndrome. PLoS One 10:e0128561

[39] Kiebish MA, Yang K, Liu X, Mancuso DJ, Guan S, Zhao Z, Sims HF, Cerqua R, Cade WT, Han X, Gross RW (2013) Dysfunctional cardiac mitochondrial bioenergetic, lipidomic, and signaling in a murine model of Barth syndrome. J Lipid Res 54:1312-1325

[40] Williamson DH, Lund P, Krebs HA (1967) The redox state of free nicotinamide-adenine dinucleotide in the cytoplasm and mitochondria of rat liver. Biochem J 103:514 – 527

[41] Gabriel JL and Plaut GW (1984). Inhibition of bovine heart NAD-specific isocitrate dehydrogenase by reduced pyridine nucleotides: modulation of inhibition by ADP, NAD+, calcium (2+), citrate, and isocitrate. Biochemistry 23:2773-2778

[42] Smith CM, Bryla J, Williamson JR (1974) Regulation of mitochondrial alpha-ketoglutarate metabolism by product inhibition at alpha-ketoglutarate dehydrogenase. J Biol. Chem 249:1497–1505

[43] Kelley RI, Cheatham JP, Clark BJ, Nigro MA, Powell BR, Sherwood GW, Sladky JT, Swisher WP (1991) X-linked dilated cardiomyopathy with neutropenia, growth retardation, and 3-methylglutaconic aciduria. J Pediatr 119:738-747

[44] Cade WT, Spencer CT, Reeds DN, Waggoner AD, O'Connor R, Maisenbacher M, Crowley JR, Byrne BJ, Peterson LR (2013) Substrate metabolism during basal and hyperinsulinemic conditions in adolescents and young-adults with Barth syndrome. J Inherit Metab Dis 36:91-101

[45] Su B and Ryan RO (2014) Metabolic biology of 3-methylglutaconic acid-uria: a new perspective. J Inherit Metab Dis 37:359–36

[46] Ikon N, Ryan RO (2016) On the origin of 3-methylglutaconic acid in disorders of mitochondrial energy metabolism. J Inherit Metab Dis 39:749-756

[47] Mamer OA, Tjoa SS, Scriver CR, Klasen GA (1976) Demonstration of a new mammalian isoleucine catabolic pathway yielding an R series of metabolites. Biochem J 160:417-426

[48] Korman SH, Andresen BS, Zeharia A, Gutman A, Boneh A, Pitt JJ (2005) 2-ethylhydracrylic aciduria in short/branched-chain acyl-CoA dehydrogenase deficiency:

application to diagnosis and implications for the R-pathway of isoleucine oxidation. Clin Chem 51:610-617

[49] Haapalainen AM, Meriläinen G, Wierenga RK (2006) The thiolase superfamily: condensing enzymes with diverse reaction specificities. Trends Biochem Sci 31:64-71

[50] Ryan, RO (2015) Metabolic annotation of 2-ethylhydracrylic acid. Clinica Chimica Acta 448:91-97

[51] Sweetman L, Weyler W, Nyhan WL, de Céspedes C, Loria AR, Estrada Y (1978) Abnormal metabolites of isoleucine in a patient with propionyl-CoA carboxylase deficiency. Biomed Mass Spectrom 5:198-207

[52] Kuhara T, Matsumoto I (1980) Studies on the urinary acidic metabolites from three patients with methylmalonic aciduria. Biomed Mass Spectrom 7:424-8

[53] Goodman SI, McCabe ER, Fennessey PV, Miles BS, Mace JW, Jellum E (1978) Methylmalonic/beta-hydroxy-n-valeric aciduria due to methylmalonyl-CoA mutase deficiency. Clin Chim Acta 87:441- 449

[54] Chicco AJ, Sparagna GC (2007) Role of cardiolipin alterations in mitochondrial dysfunction and disease. Am J Physiol Cell Physiol 292:C33-44

[55] Shen Z, Ye C, McCain K, Greenberg ML (2015) The Role of Cardiolipin in Cardiovascular Health. Biomed Res Int 2015:Article ID 891707

[56] Lesnefsky EJ, Chen Q, Hoppel CL (2016) Mitochondrial Metabolism in Aging Heart. Circ Res 118:1593-1611

[57] Towbin JA, Lorts A, Jefferies JL (2015) Left ventricular non-compaction cardiomyopathy. Lancet 386:813-825

[58] Spencer CT, Bryant RM, Day J, Gonzalez IL, Colan SD, Thompson WR, Berthy J, Redfearn SP, Byrne BJ (2006) Cardiac and clinical phenotype in Barth Syndrome. Pediatrics 118:e337-e346

[59] Guertl B, Noehammer C, Hoefler G (2000) Metabolic cardiomyopathies. Int J Exp Pathol 81:349–372

[60] Debold EP, Schmitt JP, Patlak JB, Beck SE, Moore JR, Seidman JG, Seidman C, Warshaw DM (2007) Hypertrophic and dilated cardiomyopathy mutations differentially affect the molecular force generation of mouse alpha-cardiac myosin in the laser trap assay. Am J Physiol Heart Circ Physiol 293:H284-291

[61] Cade WT, Reeds DN, Peterson LR, Bohnert KL, Tinius RA, Benni PB, Byrne BJ, Taylor CL (2016) Endurance Exercise Training in Young Adults with Barth Syndrome: A Pilot Study JIMD Rep Jun 11 [Epub ahead of print]

[62] Janz, KF, Dawson JD, Mahoney LT. (2000) Predicting heart growth during puberty: the Muscatine Study. Pediatrics, 105: e63.

[63] Wang Z, Ying Z, Bosy-Westphal A, Zhang J, Schautz B, Later W, Heymsfield SB, Müller MJ. (2010) Specific metabolic rates of major organs and tissues across adulthood: evaluation by mechanistic model of resting energy expenditure. American

journal of clinical nutrition. 92:1369-77.

[64] Valianpour F, Wanders RJ, Overmars H, Vaz FM, Barth PG, van Gennip AH. (2003) Linoleic acid supplementation of Barth syndrome fibroblasts restores cardiolipin levels: implications for treatment. J. Lipid Res. 44; 560-566.

Chapter 2: Cardiolipin Nanodisks Deliver Cardiolipin to Mitochondria and Prevent TAZ Knockdown-Induced Apoptosis in Myeloid Progenitor Cells

Introduction

Cardiolipin (CL) is a unique, highly specialized phospholipid that differs from other glycerophospholipids in that it contains four fatty acyl chains and three glycerol moieties, giving rise to a negatively charged, cone-shaped structure. In animals, CL is found almost exclusively in mitochondria, mostly on the matrix side of the inner membrane [1] where it interacts with, and stabilizes, electron transport chain (ETC) proteins. CL binds tightly to proteins that participate in oxidative phosphorylation including complex IV [2], ATP/ADP exchange protein [3], F_0F_1 ATP synthase [4], the orthophosphate transporter [5] and the cytochrome bc_1 complex [6]. Moreover, CL binding is also necessary for optimal activity of complex IV [2], complex I and complex III [7]. CL is also required for ADP/ATP carrier function and formation of ETC supercomplexes [8-11].

Reduced levels of CL are associated with a number of common conditions, including age-related heart failure [12-14] and diabetes [15]. Profound defects in CL content and composition are a feature of Barth Syndrome (BTHS), a rare, life threatening X-linked disorder caused by loss of function mutations in the tafazzin gene (*TAZ;* OMIM entry *300394) [16]. *TAZ* encodes a phospholipid transacylase that localizes to mitochondria and functions in CL acyl chain remodeling [17]. BTHS patients are characterized by decreased amounts of CL, particularly in cardiac and skeletal muscle, altered CL molecular species composition and an increase in the ratio of monolyso CL / CL [18]. These alterations in CL lead to severe muscle weakness and cardiomyopathy, which can lead to heart failure, one of the leading causes of death among BTHS patients [19].

In addition to cardiomyopathy and skeletal muscle weakness, BTHS is characterized by neutropenia [19]. As neutrophils are the primary phagocytic cells of the human immune system, their depletion predisposes BTHS patients to infection. Based on their short half-life (~24 h) and relatively high abundance in circulation, the turnover rate of neutrophils is high. Thus, defective maturation can lead to a sharp decline in the concentration of circulating neutrophils. Makaryan et al [20] showed that HL60 myeloid progenitor cells transfected with a *TAZ*-specific shRNA undergo apoptosis. Based on this, it was proposed that neutropenia in BTHS arises from increased apoptosis of neutrophil precursor cells. In the present study, we employed HL60 cells to evaluate the ability of exogenous CL to prevent the apoptotic phenotype induced by *TAZ* knockdown. The data indicate that CL, solubilized in nanodisk (ND) complexes, is taken up, localizes to mitochondria, and prevents *TAZ* knockdown-induced apoptosis.

Materials and Methods

Formulation of CL-ND. Tetralinoleoylcardiolipin [$(18:2/18:2)_2$-cardiolipin] and tetra-myristoylcardiolipin [$(14:0/14:0)_2$-cardiolipin] were purchased from Avanti Polar Lipids. Five mg of a given CL (stock solution in chloroform) was transferred to a glass tube and the solvent evaporated under a stream of N_2 gas. Residual solvent was removed under vacuum. The prepared lipid was dispersed in phosphate buffered saline (PBS; 20 mM sodium phosphate, 150 mM sodium chloride, pH 7.0) followed by the addition of 2 mg recombinant human apoA-I [21] in a final volume of 1mL. The sample was subjected to bath sonication under a N_2 atmosphere, with the temperature maintained between 22°C

and 25°C. During sonication, the turbid lipid dispersion became clear indicating apolipoprotein/phospholipid complexes (i.e. CL-ND) had formed. No pellet formed upon centrifugation. Control ND, containing dimyristoyl-phosphatidylcholine (Avanti Polar Lipids), were prepared in a similar manner. Where indicated, CL-ND were formulated in the presence (1 % w/w) of a flourescent CL (TopFlour-Cardiolipin; Avanti Polar Lipids)]

Electron Microscopy. A drop of freshly prepared CL-ND was deposited on a carbon-coated grid and, after 15 sec, excess fluid was wicked away and a solution of 2% potassium phosphotungstate (pH 6.5) added. Excess stain was removed and the grid air-dried. Grids were examined at 80 kV in a JEM-1230 electron microscope (JEOL, Peabody, MA), and imaged with an UltraScan™ USC1000 charge-coupled device camera (Gatan, Warrendale, PA). Particle diameters were measured according to Forte and Nordhausen [22].

HL60 cell culture. Human HL60 promyelocytic leukemia cells were obtained from ATCC and cultured in RPMI 1640 media supplemented with 10% fetal bovine serum, 100 µg/mL penicillin, and 100 µg/mL streptomycin at 37°C in a humidified atmosphere of 5% CO_2. The cells were passaged every 3-4 days.

Cardiolipin uptake studies. HL60 cells (2×10^6) were incubated with PBS or tetralinoleoyl CL-ND (750 µg CL) in serum free medium for 24 h at 37°C. Following incubation, cells were washed and 100 µg of butylated hydroxytoluene and 5 µg tetramyristoyl CL (internal standard) were added. Cells were extracted according to Bligh and Dyer [23] with modifications of Garrett et al [24].

Liquid chromatography – mass spectrometry (LC-MS). Negative ion electrospray ionization (ESI) LC-MS analysis of extracted CL was conducted on a Thermo Scientific (San Jose, CA) Vantage TSQ mass spectrometer with Thermo Accela UPLC operated by Xcalibur software. Separation of lipid was achieved by a Restek 150 x 2.1 mm (5 µm particle size) Viva C4 column at a flow rate of 260 µL/min. The mobile phase contained 10 mM ammonium formate in solvent A: acetonitrile:water (60:40, v:v); solvent B: 2-propanol:acetonitrile (90:10, v:v); and a gradient elution in the following manner was applied: 68% A, 0-1.5 min; 68-55% A, 1.5-4 min; 55-48% A, 4-5 min; 48-42% A, 5-8 min; 42-34% A, 8-11 min; 34-30% A, 11-14 min; 30-25% A, 14-18 min; 25-3% A, 18-23 min; 3-0% A, 25-30 min and kept at 0% A for 5 min. The tetramyristoyl CL internal standard (m/z 1240, $[M - H]^-$) was eluted at 13.6 min, and the tetralinoleoyl CL (m/z 1448, $[M - H]^-$) eluted at 14.4 min. Calculation of tetralinoleoyl CL content was based on the ratio of peak area of $(18:2/18:2)_2$-CL and $(14:0/14:0)_2$-CL from lipid extracts of cells incubated with PBS and CL-ND.

Confocal microscopy. HL60 cells (2 x 10^6) were incubated (24 h at 37°C) in 6 well plates containing poly-L-lysine-treated coverslips (BD Biosciences) in the presence of CL-ND (100 µg tetralinoleoyl CL + 1 µg TopFluor-CL). Following incubation, cells were washed with PBS and incubated with Mitotracker Orange (Life Technologies) according to the manufacturer's protocol, and fixed with 4% paraformaldehyde (prepared in PBS containing 0.03 M sucrose) for 15 min at 22 °C. Hoechst 33342 was employed as a nuclear stain. Cells were mounted on microscope slides, sealed with nail polish, and visualized at 63X with the Zeiss LSM710 confocal microscope.

TAZ knockdown experiments. HL60 cells (2 x 10^5) were seeded 2 days before the planned experiment. Cells were pelleted and re-suspended in nucleofection buffer containing 60 pmoles *TAZ* specific siRNA or a scrambled siRNA (Santa Cruz Biotechnology). The samples were electroporated with an Amaxa Cell Line Nucleofector Kit V, transferred to a 12 well plate at 1 x 10^6 cells/well and cultured in complete medium for 24 h. Where indicated, the media was supplemented with CL-ND (100 µg CL). Although nucleofection causes significant background apoptosis in this cell type, it remains the most effective method for HL60 cell transfection [25].

Reverse Transcriptase (RT)-PCR. Cells were processed with an Aurum Total RNA isolation kit (Bio-Rad) according to the manufacturer's protocol. RT-PCR was performed using TaqMan PCR Reagent Kit (Applied Biosystems) and SYBR Green PCR Master Mix (Applied Biosystems). Primers specific for *TAZ* or *GAPDH* were employed, as described by Makaryan et al [20]. qPCR was performed using an Applied Biosystems 7900HT Fast Real-Time PCR System. Cycle threshold values derived from qPCR analysis were normalized to GAPDH mRNA levels.

Apoptosis studies. Following incubation in the presence or absence of CL-ND, *TAZ* knockdown and control HL60 cells were incubated with a) Alexa Fluor 488-labeled annexin V (Invitrogen) or b) propidium iodide (PI), as reported by Riccardi and Nicoletti [26]. In both assays, the cells were subject to flow cytometry analysis on a BD LSRFortessa and the data processed using FlowJo software]

Results

Effect of apoA-I on CL solubility. When 5 mg tetralinoleoyl CL was dispersed in PBS and bath sonicated, the sample remained turbid (**Figure 1A**). However, when CL was dispersed in PBS containing 2 mg recombinant human apoA-I, sample light scattering intensity was dramatically decreased. The extent of sample clarification was similar to that previously observed for phosphatidylcholine (PC) [27], indicating that CL behaves in a similar manner. The morphology of the complexes generated was examined by

negative stain electron microscopy (**Figure 1B**), revealing a population of ND particles (seen en face) with diameters ranging from 18 to 31 nm.

*Uptake of CL-ND by HL60 cells***.** To assess if CL-ND can serve as a vehicle for delivery of CL to cells in culture, HL60 cells were incubated with tetralinoleoyl CL-ND. After 24 h, the cells were extracted and CL analyzed by LC-MS. In control cell extracts, the peak corresponding to the internal standard (tetramyristoyl CL) was prominent, while the peak corresponding to native tetralinoleoyl CL was just above background (**Figure 2A**). Upon treatment with CL-ND, however, the peak corresponding to tetralinoleoyl CL increased (**Figure 2C**). Similarly, an averaged spectrum view of control cell extracts shows a tetralinoleoyl CL peak that is low relative to the internal standard (**Figure 2B**), while in CL-ND treated cell extracts, this peak increased (**Figure 2D**). Peak quantification, relative to the internal standard, shows that, following incubation with CL-ND, the cellular content of tetralinoeoyl CL increased 30 fold (**Figure 2E).**

Exogenous CL homes to mitochondria. While the results presented above show CL uptake by HL60 cells, we sought to determine its intracellular fate following uptake. Cells were incubated with CL-ND containing small amounts of a fluorescent CL analogue and subjected to confocal fluorescence microscopy. Micrographs depicted in **Figure 3** reveal a strong, punctate, perinuclear pattern of CL fluorescence within the cell and minor fluorescence associated with the plasma membrane. The punctate CL fluorescence signal co-localized with fluorescence derived from the mitochondria-specific reagent, MitoTracker, indicating exogenous CL localization to mitochondria.

Effect of CL-ND on TAZ knockdown-induced annexin V binding to HL60 cells. Compared to cells treated with a scrambled siRNA, *TAZ* specific siRNA induced a ~50% decline in *TAZ* mRNA levels (data not shown). To evaluate the effect of *TAZ* knockdown on HL60 cell apoptosis, cell surface exposure of phosphatidylserine was measured by flow cytometry following incubation with AlexaFluor 488-labeled annexin V. Consistent with results reported earlier [20], *TAZ* knockdown induced an increase in annexin V binding relative to cells treated with a scrambled siRNA (**Figure 4A**). Incubation of *TAZ* knockdown cells with CL-ND decreased annexin V binding to levels similar to that observed for cells treated with scrambled siRNA plus CL-ND, suggesting that CL-ND treatment prevents *TAZ* knockdown-induced apoptosis.

Effect of TAZ knockdown on PI staining of HL60 cells. To confirm the effect of CL-ND treatment on *TAZ* knockdown HL60 cells, an independent apoptosis assay, based on DNA degradation, was employed. Compared to cells treated with scrambled siRNA, *TAZ* siRNA-treated cells showed increased apoptosis (**Figure 4B**). Incubation of *TAZ* siRNA-treated cells with CL-ND eliminated this increase, while incubation of scrambled siRNA-treated cells with CL-ND had no significant effect, confirming that CL-ND treatment prevents *TAZ* knockdown-induced apoptosis.

Discussion

Reconstituted high-density lipoprotein (rHDL) are readily formed by combining glycerophospholipids, such as PC, with an apolipoprotein. Many different apolipoproteins, fragments thereof or synthetic peptides, possess the ability to form rHDL. In general, the particles created exist as nanoscale, disk-shaped phospholipid bilayers whose periphery is circumscribed by two or more apolipoprotein molecules. The protein/peptide “scaffold” of rHDL functions to stabilize the otherwise unstable edge of the phospholipid bilayer. Because different combinations of lipid and apolipoprotein can be used to formulate unique rHDL, this technology has been exploited for applications well beyond lipoprotein metabolism [27,28]. To distinguish rHDL engineered to possess additional features (e.g. inclusion of a hydrophobic drug), the term nanodisk (ND) is used.

In the present study, ND were formulated using CL. CL is different from other glycerophospholipids in that two acylated phosphoglycerol backbones share a third glycerol moiety as head group, giving rise to a distinctly cone-shaped anionic phospholipid possessing four esterified fatty acyl chains. In eukaryotes, CL is mainly confined to the inner membrane of mitochondria where it plays a key role in energy metabolism by establishing an optimal membrane environment for ETC proteins [29]. As such, defects in CL content and composition compromise mitochondrial function. In tissues with high oxidative metabolic capacity, including cardiac and skeletal muscle, CL fatty acyl chains are remodeled by the transacylase tafazzin to generate tetralinoleoyl CL as the major molecular species (> 90 %). It is conceivable that attainment of this fatty acyl chain composition enhances lipid packing, thereby establishing a membrane environment that facilitates optimal conditions for electron flux, generation / maintenance of a proton gradient, and ATP production. Indeed, individuals with BTHS harbor mutations in *TAZ* and display alterations in CL molecular species composition, decreased CL levels and increased amounts of monolyso-CL [19]. Similarly, CL-deficient mitochondria, isolated from hypothyroid patients, manifest impaired oxidative function [30]. Interestingly, treatment of isolated mitochondria from these subjects with exogenous CL restored normal activity. In cultured BTHS fibroblasts, linoleic acid supplementation of growth medium led to a time and dose dependent restoration of total CL levels and a significant increase in tetralinoleoyl CL [31]. Thus, it is conceivable that tafazzin-dependent CL remodeling can be bypassed by increasing substrate availability for direct *de novo* synthesis of tetralinoleoyl CL or by provision of exogenous tetralinoleoyl CL directly to the mitochondria.

Herein, it was hypothesized that the requirement for a functional tafazzin protein could be lessened or circumvented if exogenous tetralinoleoyl CL was provided to cultured cells. The work of Makaryan et al [20] established a cell culture model of BTHS neutropenia in which the functional effects of this hypothesis can be tested. The current study confirms that *TAZ* knockdown induces apoptosis. Moreover, we show that incubation of *TAZ* knockdown cells with CL-ND attenuates their apoptotic response. The lack of complete inhibition observed in annexin V binding assays is likely an artifact caused by annexin V recognition of CL [32] retained in the plasma membrane following incubation with CL-ND. To control for this, an independent, DNA quantification-based, PI

binding apoptosis assay was performed [26]. The results of this assay confirm that incubation of *TAZ* knockdown HL60 cells with CL-ND attenuates their apoptotic response.

Although the present HL60 cell culture model of BTHS fails to manifest detectable changes in the monolyso CL / CL ratio typically associated with BTHS [20], this may be attributed to a high sensitivity of this cell type to mitochondrial dysfunction, resulting in apoptosis in response to minor changes in CL composition. Unlike muscle tissue, neutrophils possess few mitochondria, and thus may be more dependent on optimal mitochondrial function [33]. As such, although skeletal muscles of BTHS patients show modestly reduced function, neutrophil progenitors are susceptible to apoptosis.

In summary, we show that exogenously provided CL is taken up by HL60 cells, migrates to mitochondria and compensate for the effects of *TAZ* knockdown. The results suggest that CL-ND have the potential to bypass *TAZ* mutations *in vivo*. Because current therapies are largely palliative, this work represents the first direct intervention for BTHS. Future studies may also reveal a potential benefit of CL-ND for age-related heart disease and other CL-associated disorders.

Based on the promising results of CL-ND treatment in cell culture, the next logical step is the evaluation of CL-ND in a mouse model of BTHS. Recently, Acehan et al. have developed a doxycycline (dox)-inducible *taz* shRNA KD mouse that recapitulates the BTHS phenotype [34]. While intact animals present a more complex drug delivery challenge, success in an animal model will pave the way for a human treatment.

Figures

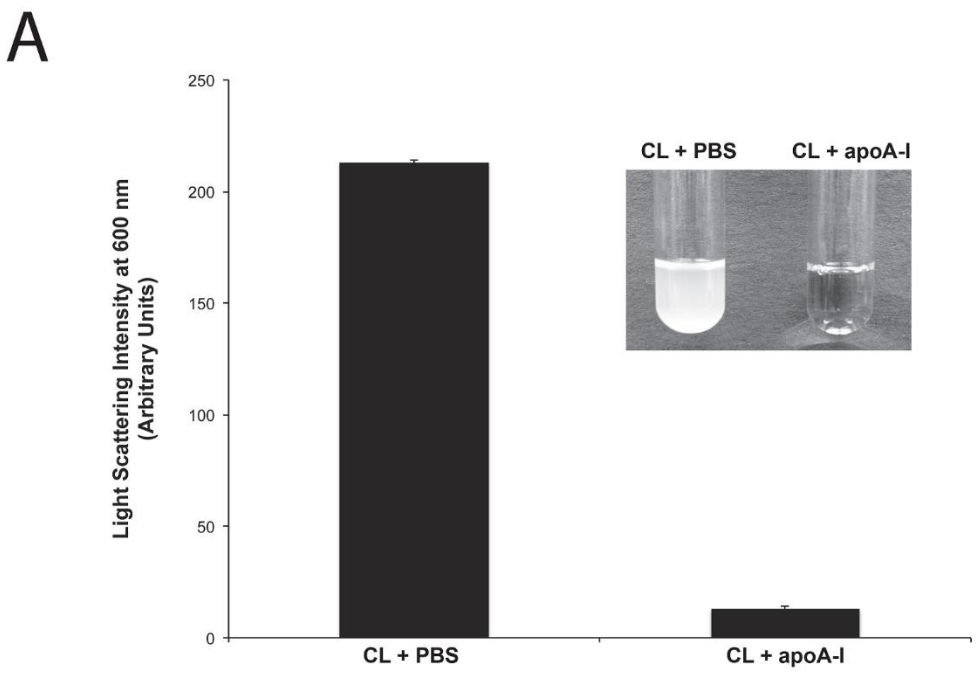

Figure 1. **Effect of apoA-I on CL solubility.** Panel A) Five mg tetralinoleoyl CL was dispersed in PBS or PBS containing 2 mg/ml apoA-I. Following bath sonication, sample light scattering intensity was measured at 600 nm on a Perkin Elmer Lamda 20 UV/Vis spectrophotometer. Inset: photographic images of the samples. Panel B) Negative stain electron microscopy of complexes generated upon incubation of CL with apoA-I in PBS. The bar represents 200 nm.

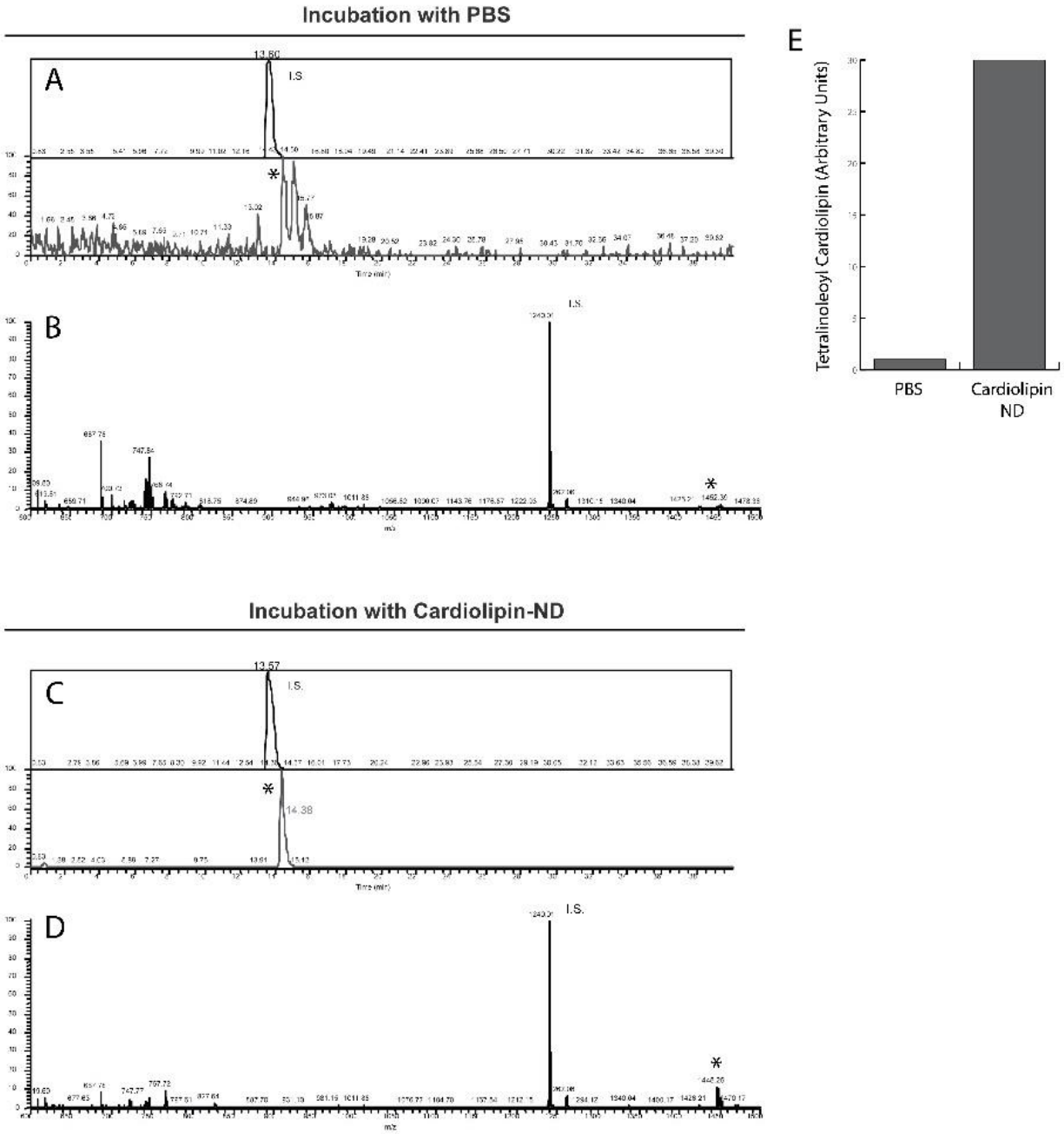
Incubation with PBS
A
I.S
B
I.S.
Incubation with Cardiolipin-ND
C
I.S.
14.38
D
I.S.
E
Tetralinoleoyl Cardiolipin (Arbitrary Units)
PBS
Cardiolipin ND

Figure 2. **LC / MS of HL60 cell extracts.** HL60 cells were incubated with PBS or PBS containing tetralinoleoyl CL-ND. Panel A) LC/MS ion chromatograms of the internal standard, tetramyristoyl CL ("I.S."; top) and of tetralinoleoyl CL (" * "; bottom) from extracts of cells incubated with PBS. Panel B) The averaged ESI/MS spectrum of material eluted between 13.36-16.36 min from extracts of cells incubated with PBS. Panel C and D) Corresponding ion chromatograms and averaged mass spectrum, respectively, of lipid extracts from cells incubated with tetralinoleoyl CL-ND. Panel E) Histogram depicting the effect of CL-ND incubation on the tetralinoleoyl CL content of HL-60 cells, relative to I.S.

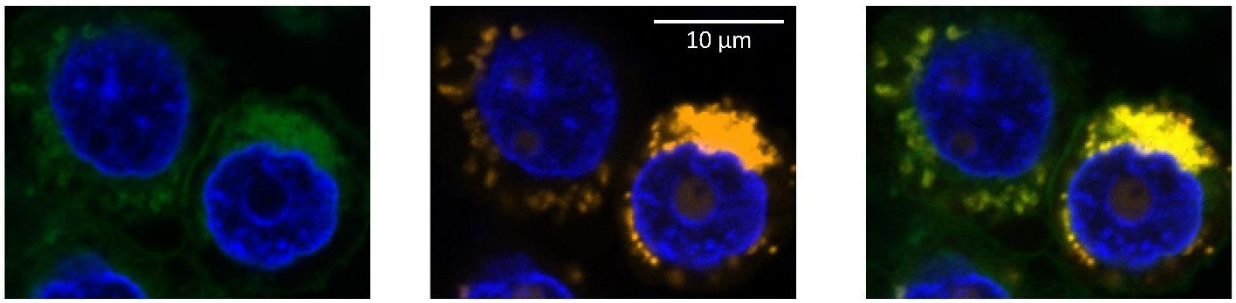

Figure 3. Confocal microscopy of HL60 cells. HL60 cells were incubated with CL-ND (100 µg tetralinoleoyl CL + 1 µg TopFluor-CL; left panel). Mitochondria were stained with MitoTracker Orange (middle panel). Nuclei were stained with Hoechst 33342. The right panel depicts a merged image with co-localization of mitochondria and TopFluor CL giving rise to a yellow fluorescence signal. Results depicted are representative images from three independent experiments.

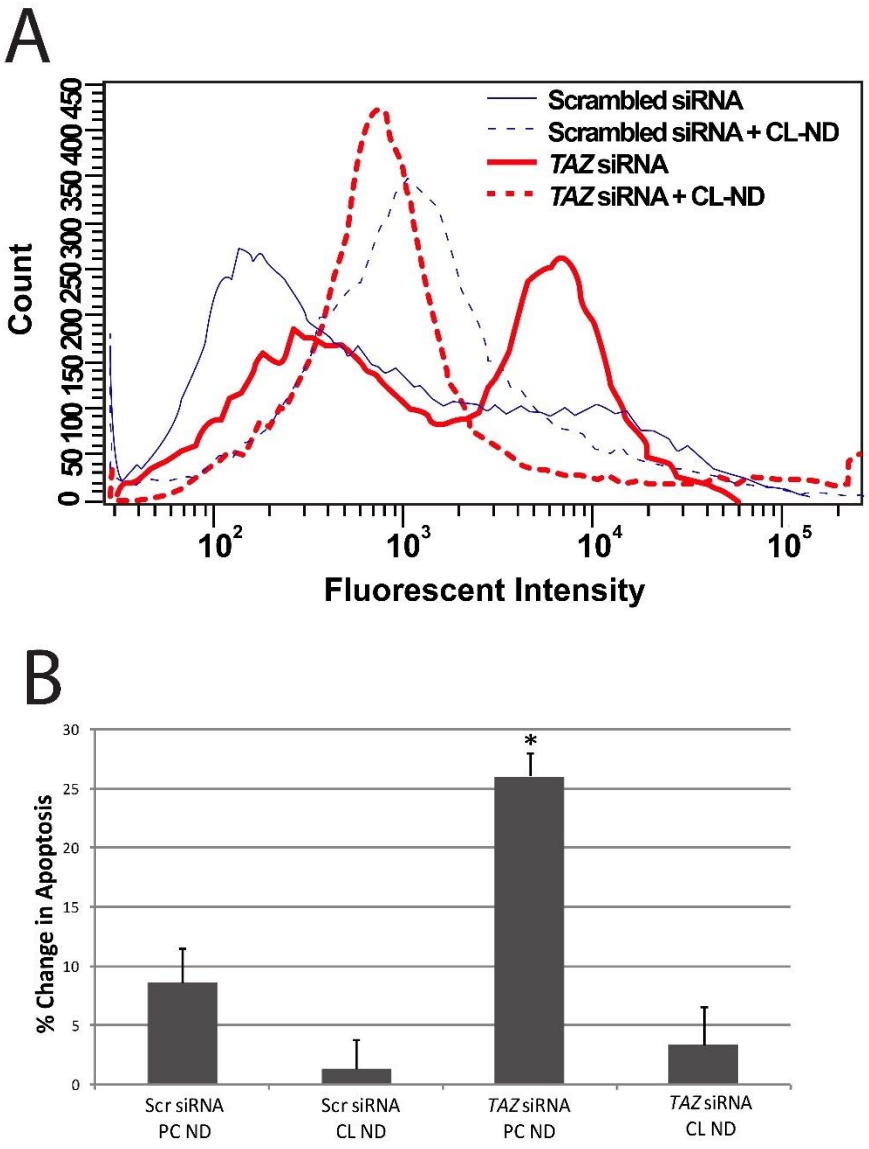

Figure 4. **Effect of CL-ND on *TAZ* knockdown-induced apoptosis in HL60 cells**. HL60 cells were electroporated in the presence of a scrambled or *TAZ*-specific siRNA. Panel A) Following electroporation, the media was supplemented with PBS alone or PBS containing tetralinoleoyl CL-ND. After 24 h incubation, the cells were probed with AlexaFluor 488-labeled annexin V and analyzed by flow cytometry. Results depicted are representative of thre\e independent experiments. Panel B) Following electroporation, the media was supplemented with PBS containing tetralinoleoyl CL-ND or PC-ND. After 24 h the cells treated with a permeabilizing PI solution and analyzed by flow cytometry. Values are the mean ± S.E. (n = 3); *P< 0.05 based on Student's T test.

References

[1] Horvath SE, Daum G (2013) Lipids of mitochondria, Prog. Lipid Res. 52: 590–614.

[2] Robinson NC, Zborowski J, Talbert LH (1990) Cardiolipin-depleted bovine heart cytochrome c oxidase: binding stoichiometry and affinity for cardiolipin derivatives, Biochemistry. 29: 8962–8969.

[3] Horváth LI, Drees M, Beyer K, Klingenberg M, Marsh D (1990) Lipid-protein interactions in ADP-ATP carrier/egg phosphatidylcholine recombinants studied by spin-label ESR spectroscopy, Biochemistry. 29:10664–10669.

[4] Eble KS, Coleman WB, Hantgan RR, Cunningham CC (1990) Tightly associated cardiolipin in the bovine heart mitochondrial ATP synthase as analyzed by 31P nuclear magnetic resonance spectroscopy, J. Biol. Chem. 265:19434–19440.

[5] Kaplan RS, Pratt RD, Pedersen PL (1989) Purification and reconstitution of the phosphate transporter from rat liver mitochondria, Methods Enzymol. 173:732–745.

[6] Yu L, Yu C, King TE (1978) The indispensability of phospholipid and ubiquinone in mitochondrial electron transfer from succinate to cytochrome c, J. Biol. Chem. 253:2657–2663.

[7] Fry M, Green DE (1981) Cardiolipin requirement for electron transfer in complex I and III of the mitochondrial respiratory chain, J. Biol. Chem. 256:1874–1880.

[8] Claypool SM, Oktay Y, Boontheung P, Loo JA, Koehler CM (2008) Cardiolipin defines the interactome of the major ADP/ATP carrier protein of the mitochondrial inner membrane, J. Cell Biol. 182:937–950.

[9] Hoffmann B, Stöckl A, Schlame M, Beyer K, Klingenberg M\ (1994) The reconstituted ADP/ATP carrier activity has an absolute requirement for cardiolipin as shown in cysteine mutants, J. Biol. Chem. 269:1940–1944.

[10] Pfeiffer K, Gohil V, Stuart RA, Hunte C, Brandt U, Greenberg ML, et al. (2003) Cardiolipin Stabilizes Respiratory Chain Supercomplexes, J. Biol. Chem. 278:52873–52880.

[11] Zhang M, Mileykovskaya E, Dowhan W (2005) Cardiolipin is essential for organization of complexes III and IV into a supercomplex in intact yeast mitochondria, J. Biol. Chem. 280:29403–29408.

[12] Paradies G, Petrosillo G, Paradies V, Ruggiero RM (2010) Oxidative stress, mitochondrial bioenergetics, and cardiolipin in aging, Free Radic. Biol. Med. 48:1286–1295.

[13] Pamplona R (2008) Membrane phospholipids, lipoxidative damage and molecular integrity: A causal role in aging and longevity, Biochim. Biophys. Acta - Bioenerg. 1777:1249–1262.

[14] Mejia EM, Nguyen H, Hatch GM (2014) Mammalian cardiolipin biosynthesis, Chem. Phys. Lipids. 179:11–16.

[15] Shi Y (2010) Emerging roles of cardiolipin remodeling in mitochondrial dysfunction associated with diabetes, obesity, and cardiovascular diseases, J. Biomed. Res. 24:6–15.

[16] Whited K, Baile MG, Currier P, Claypool SM (2013) Seven functional classes of barth syndrome mutation, Hum. Mol. Genet. 22:483–492.

[17] Xu Y, Malhotra A, Ren M, Schlame M (2006) The enzymatic function of tafazzin, J. Biol. Chem. 281:39217–39224.

[18] Valianpour F, Wanders RJA, Barth PG, Overmars H, Van Gennip AH (2002) Quantitative and compositional study of cardiolipin in platelets by electrospray ionization mass spectrometry: Application for the identification of Barth syndrome patients, Clin. Chem. 48:1390–1397.

[19] Clarke SLN, Bowron A, Gonzalez IL, Groves AJ, Newbury-Ecob N, Clayton N, et al. (2013) Barth syndrome, Orphanet J. Rare Dis. 8:23.

[20] Makaryan V, Kulik W, Vaz FM, Allen C, Dror Y, Dale DC, et al. (2012) The cellular and molecular mechanisms for neutropenia in Barth syndrome, Eur. J. Haematol. 88:195–209.

[21] Ryan RO, Forte TM, Oda MN (2003) Optimized bacterial expression of human apolipoprotein A-I, Protein Expr. Purif. 27:98–103.

[22] Forte TM, Nordhausen RW (1986) Electron microscopy of negatively stained lipoproteins, Methods Enzymol., 442–457.

[23] Bligh EG, Dyer WJ (1959) A rapid method of total lipid extraction and purification, Can. J. Biochem. Physiol. 37:911–917.

[24] Garrett TA, Kordestani R, Raetz CRH (2007) Quantification of Cardiolipin by Liquid Chromatography-Electrospray Ionization Mass Spectrometry, Methods Enzymol. 433:213–230.

[25] Schakowski F, Buttgereit P, Mazur M, Märten A, Schöttker B, Gorschlüter M, et al. (2004) Novel non-viral method for transfection of primary leukemia cells and cell lines, Genet. Vaccines Ther. 2:1

[26] Riccardi C, Nicoletti I (2006) Analysis of apoptosis by propidium iodide staining and flow cytometry, Nat. Protoc. 1:1458–61.

[27] Ryan RO (2008) Nanodisks: hydrophobic drug delivery vehicles, Expert Opin. Drug Deliv. 5:343–351.

[28] Ryan RO (2010) Nanobiotechnology applications of reconstituted high density lipoprotein, J. Nanobiotechnology. 8:28.

[29] Houtkooper RH, Vaz FM (2008) Cardiolipin, the heart of mitochondrial metabolism, Cell. Mol. Life Sci. 65:2493–2506.

[30] Paradies G, Petrosillo G, Paradies V, Ruggiero FM (2009) Role of cardiolipin peroxidation and Ca2+ in mitochondrial dysfunction and disease, Cell Calcium. 45:643–650.

[31] Valianpour F, Wanders RJ, Overmars H, Vaz FM, Barth PG, van Gennip AH (2003) Linoleic acid supplementation of Barth syndrome fibroblasts restores cardiolipin levels: implications for treatment, J. Lipid Res. 44:560–566.

[32] Megli FM, Selvaggi M, De Lisi A, Quagliariello E (1995) EPR study of annexin V-cardiolipin Ca-mediated interaction in phospholipid vesicles and isolated mitochondria, Biochim. Biophys. Acta - Biomembr. 1236:273–278.

[33] van Raam BJ, Kuijpers TW (2009) Mitochondrial defects lie at the basis of neutropenia in Barth syndrome, Curr. Opin. Hematol. 16:14–19.

[34] Acehan D, Vaz F, Houtkooper RH, James J, Moore V, Tokunaga C, Kulik W, Wansapura J, Toth MJ, Strauss A, Khuchua Z. (2011) Cardiac and skeletal muscle defects in a mouse model of human Barth syndrome. J. Biol. Chem. 286; 899-908.

Chapter 3: Evaluation of Cardiolipin Nanodisks as a Lipid Replacement Therapy in a Mouse Model of Barth Syndrome

Introduction

Barth Syndrome (BTHS) is a rare, life threatening X-linked recessive disorder characterized by cardiomyopathy, skeletal muscle weakness, low weight gain, neutropenia, and 3-methylglutaconic aciduria[1]. The underlying cause of BTHS has been traced to mutations in the tafazzin (*TAZ*) gene[2, 3], which encodes a phospholipid transacylase, termed tafazzin[4]. Loss of tafazzin activity leads to a deficiency in cardiolipin (CL), an important phospholipid component of the inner mitochondrial membrane (IMM). Additional changes include increased CL molecular species heterogeneity and accumulation of monolyso (ML) CL[5]. Given the key structural role CL plays in the IMM [6], it is not surprising that BTHS subjects manifest ultrastructural changes to this organelle[7], as well as defective energy metabolism, particularly in cardiac tissue and skeletal muscle[8]. Normally, heart and skeletal muscle mitochondria are highly enriched in a single CL molecular species, tetralinoleoyl CL[9]. Establishment and maintenance of this molecular species composition is dependent upon acyl chain remodeling reactions that involve tafazzin transacylase activity[10]. When tafazzin is missing or defective, major changes in CL content and composition occur.

To date, treatment of BTHS is largely symptomatic and directed toward alleviating problems associated with cardiomyopathy, skeletal myopathy and neutropenia. However, earlier research suggests that compensating for defective tafazzin activity may be a feasible approach. For example, Valianpour et al. [11] investigated whether linoleic acid supplementation of the growth medium for cultured BTHS fibroblasts would have an effect on tetralinoleoyl CL levels. These authors reported a time and dose dependent increase in tetralinoleoyl CL following supplementation with linoleic acid, suggesting that a deficiency in tafazzin-mediated CL remodeling can be bypassed by increasing substrate availability for direct *de novo* synthesis of tetralinoleoyl CL.

To investigate the underlying cause of neutropenia in BTHS, Makaryan et al[12] used HL60 myeloid progenitor cells as a model system. When these cells were transfected with a *TAZ*-specific short-hairpin RNA (shRNA), increased apoptosis was observed. Subsequently, in an attempt to bypass the deficiency, TAZ knockdown (KD) HL60 cells were incubated with CL nanodisks (ND), water soluble nanoscale particles formed upon incubation of an aqueous dispersion of tetralinoleoyl CL with an amphipathic apoliporotein[13-15]. ND-mediated delivery of tetralinoleoyl CL to cultured *TAZ* KD HL60 cells delivered exogenous CL to mitochondria and attenuated the apoptotic response [15].

Based on these *in vitro* results, it was hypothesized that *in vivo* administration of CL-ND may affect mitochondrial CL levels. A doxycycline (dox)-inducible *taz* shRNA KD mouse has been reported that recapitulates the BTHS phenotype. These mice exhibit an abnormal CL profile, mitochondrial structural abnormalities, impaired weight gain and adult-onset cardiomyopathy[16-18]. Acehan et al. [16] observed that, at eight weeks of age, a dramatic decrease in CL content in cardiac and skeletal muscle as well as a shift toward saturated CL molecular species was seen in the mice. There was also a substantial increase in levels of monolyso cardiolipin (MLCL), resulting in an elevated MLCL/CL ratio. Pronounced defects in both cardiac and skeletal muscle were noted at eight months, including extreme morphological changes in mitochondria and severe left

ventricular dysfunction. Taken together, this murine model of BTHS recapitulates phenotypic features of the human disorder. Herein, these mice were employed in experiments designed to test the hypothesis that administration of CL-ND over a 10 week period normalizes the content and composition of CL in key tissues and, thereby, confers protection against manifestation of the BTHS disease phenotype.

Materials and Methods

CL-ND formulation: Five mg tetralinoleoyl CL [$(18:2)_4$-CL] (Avanti Polar Lipids Inc) was transferred to a glass tube and solvent evaporated under a stream of N_2 gas, forming a thin film on the vessel wall. Residual solvent was removed under vacuum. The prepared lipid was dispersed in PBS (20 mM sodium phosphate, 150 mM sodium chloride, pH 7.0) followed by the addition of 2 mg recombinant murine apolipoprotein (apo) A-I[19] in a final volume of 0.55 mL. Bath sonication of the turbid CL-apoA-I mixture induced sample clearance, an indication that CL-ND had formed[15]. CL-ND preparations were sterile-filtered (0.22 μm) prior to administration to mice.

Animals: C57BL/6J *taz* shRNA KD mice and wild type (WT) littermates were obtained from The Jackson Laboratory. WT female and hemizygous male *tet*-on shRNA KD mice were used for breeding. Breeding females were maintained on dox (625 mg/kg in chow) from one week before mating until pups were weaned, except during breeding, to prevent dox-related infertility in breeding males. Upon weaning, pups were placed on dox for the remainder of the study]

CL-ND toxicity testing: WT C57BL/6 mice were administered a single intraperitoneal (IP) injection of 0, 30, 60, 90, or 150 mg/kg CL in the form of CL-ND. After 24 h, blood was collected by submandibular vein bleed, centrifuged at 8,000g at 4°C for 10 min; plasma was recovered and stored at -80 °C until use. Analysis of plasma alanine transaminase (ALT) and aspartate transaminase (AST) activity, as well as determination of creatinine and blood urea nitrogen (BUN) levels, were performed by the UC Davis Comparative Pathology Laboratory]

CL-ND injection studies: Only male mice were used in experiments and all were maintained on dox throughout the treatment period. CL-ND administration was by IP injection, starting when pups reached 4 weeks of age and continued for 10 weeks. At the conclusion of the experiment, mice were euthanized, tissues harvested and frozen (-80°C) until extracted. The animal protocol employed was approved by Children's Hospital Oakland Research Institute's Institutional Animal Care and Use Committee. Five groups of mice were injected as follows: Group 1: *taz* shRNA KD mice (n=6) administered a weekly bolus injection of 90 mg/kg CL (as ND). Group 2: *taz* shRNA KD mice (n=6) administered a daily injection (5 days per week) of 18 mg/kg CL (as ND). Group 3: *taz*

shRNA KD mice (n=5) administered a weekly injection of PBS (corresponding to the volume of the CL-ND injection). Group 4: WT mice (n=6) administered a weekly bolus injection of 90 mg/kg CL (as ND). Group 5: WT mice (n=6) administered a weekly injection of PBS (corresponding to the volume of the CL-ND injection). Mice were weighed weekly and monitored for outward signs of health over the course of the treatment period.

Extraction of CL from tissues: Previously frozen heart, and skeletal muscle, and liver tissues were homogenized using a FastPrep FP120 Cell Disruptor and Lysing Matrix M (MP Biomedicals), according to the manufacturer's instructions. Homogenates were further disrupted by sonication and extracted as previously described[15]. Tetramyristoyl CL was used as internal standard (heart = 10 µg, muscle/liver = 1 µg)

Liquid chromatography/mass spectrometry (LC/MS) analysis: Negative ion electrospray ionization (ESI) LC/MS analysis of lipid extracts was performed on a Thermo Scientific (San Jose, CA) Vantage TSQ mass spectrometer with Thermo Accela UPLC operated by Xcalibur software. Lipids were separated on a Restek 150 x 2.1 mm (5 µm particle size) Viva C4 column under established conditions. The tetramyristoyl CL internal standard (m/z 1240, [M – H]-) elutes at 13.6 min while tetralinoleoyl CL (m/z 1448, [M – H]-) elutes at 14.4 min. Complete details of CL analysis by LC/MS are provided elsewhere[20-23].

Statistical analysis: Statistical analyses were performed using the Student's *t*-test and data are shown as mean ± SEM where $P \leq 0.05$ is considered significant.

Results

Single dose CL-ND toxicity study: To identify a safe, nontoxic dose of CL-ND, WT mice were subjected to a single injection protocol. Groups of 5 mice each were injected with 0, 30, 60, 90 and 150 mg/kg CL as CL-ND. After 24 h, plasma was obtained and analyzed for evidence of kidney and liver toxicity (**Figure 1**). Plasma levels of the liver enzymes, ALT and AST, were within the normal range at all CL concentrations tested. However, at the highest dose administered (150 mg/kg CL), a trend towards increased activity for both enzymes was noted, suggesting a liver toxicity threshold. At the same time, no CL concentration-dependent differences were observed in the levels of creatinine or BUN and all values were within the normal range, consistent with normal kidney function. Based on these findings, a dose of 90 mg/kg CL, in the form of ND, was employed in subsequent studies.

CL-ND administration to taz shRNA KD mice: Two approaches to CL-ND administration were employed. In the first, a single weekly dose of 90 mg/kg was injected IP, while the second approach employed 5 daily injections of 18 mg/kg CL-ND IP. Groups of *taz* shRNA

KD mice received a) daily or b) weekly injections of CL-ND for 10 weeks while control *taz* shRNA KD mice received weekly injections of PBS. WT mice were administered either PBS or CL-ND. Over the 10-week treatment period, mice were monitored for activity and outward signs of ill health. No significant differences in activity between groups were detected by visual comparison, and for the first 8 weeks of the treatment phase, all mice appeared healthy. However, during the final 2 weeks of treatment, three *taz* shRNA KD mice in the 90 mg/kg CL-ND weekly bolus treatment group died, two at week 9 and the third at week 10. Thus, in this treatment group, only 50% of the mice survived the 10-week treatment phase. On the other hand, all mice in the daily injection group (18 mg CL/kg/day) survived the treatment phase and appeared healthy throughout. Based on this discrepancy, it may be concluded that daily dosing is better tolerated than a single weekly bolus injection.

From the outset, *taz* shRNA KD mice were smaller and weighed less than control WT C57BL/6J mice and this difference in weight persisted throughout the treatment phase of the experiment (**Figure 2**). On average, *taz* shRNA KD mice weighed 16% less than their WT littermates ($P<0.0005$). Although no mortality was observed in WT C57BL/6J mice administered a 90 mg/kg weekly bolus of CL-ND, a trend toward reduced weight gain over time was observed. In the case of WT mice, the only CL-ND injection group received 90 mg/kg per week. Thus, it remains unclear if a daily injection protocol would have the same effect on weight gain in WT mice.

CL levels in key tissues: After 10 weeks of treatment, mice were sacrificed and tissues were harvested, flash frozen and stored at -80°C until extraction and analysis by LC/MS. Consistent with known effects of *taz* KD, heart, muscle, and liver tissue of *taz* shRNA KD mice had a significantly higher ratio of MLCL/CL, as compared to the same tissues from WT mice (**Figure 3A-C**). However, CL-ND treatment, either as a weekly bolus injection or daily injection, failed to induce a change in the MLCL / CL ratio in tissues from WT or *taz* shRNA KD mice. Absolute levels of tetralinoleoyl CL followed a similar pattern (**Figure 3D-E**).

Discussion

ND technology has been exploited for numerous applications, including packaging transmembrane proteins in a native-like membrane environment, solubilization of hydrophobic biomolecules, and as a transport vehicle for contrast agents used in magnetic resonance imaging of atherosclerotic lesions[14]. Recently, ND have been shown to be an effective means to solubilize CL[15]. Negative stain electron microscopy revealed that tetralinoleoyl CL-ND are discoidal particles with a diameter in the range of 18–31 nm. Thus, stable, water-soluble CL-ND can be generated via a facile one-step formulation process.

Makaryan et al. [12] reported that shRNA-mediated KD of *TAZ* in HL60 myeloid

progenitor cells leads to induction of apoptosis. Ikon et al. [15] confirmed this effect but also found that incubation of these cells with exogenous tetralinoleoyl CL-ND attenuates the apoptotic response. When HL60 cells were incubated with CL-ND harboring trace amounts of a fluorescent CL analogue, it was determined that exogenous CL localizes to mitochondria. These results suggest that exogenous tetralinoleoyl CL, solubilized in ND, is taken up by HL60 cells and utilized in lieu of *de novo* synthesized and/or remodeled cardiolipin. The cell culture studies also suggested that CL-ND have the capability to deliver CL to cells *in vivo* and, thus, may have therapeutic potential.

The goal of the present study was to extend these *in vitro* findings to an *in vivo* setting, with a view to CL replacement therapy as a treatment strategy for BTHS. Studies were performed using the dox-inducible *taz* shRNA KD mouse[16], which manifests BTHS-associated CL abnormalities within 8 weeks. Following identification of an optimal CL-ND dose, a 10 week study was conducted to assess the effect of CL-ND administration on: (1) the ratio of MLCL / CL and (2) the abundance of CL in key tissues. The results of LC/MS analysis indicate CL-ND administration does not alter the aberrant CL profile of *taz* shRNA KD mice. Given the relatively high dose of CL administered (90 mg/kg per week), it is unlikely that increasing CL-ND concentration, frequency of administration, or duration of treatment will overcome the transport impediment that prevents exogenously administered CL from reaching mitochondria *in vivo*. These results highlight the difficulties inherent in extrapolation of results from cell culture studies to intact animals. Based on the results obtained in this mouse model of BTHS, we conclude that administration of CL-ND, in its current form, is not a viable therapy option for treatment of this rare mitochondrial disorder.

Figures

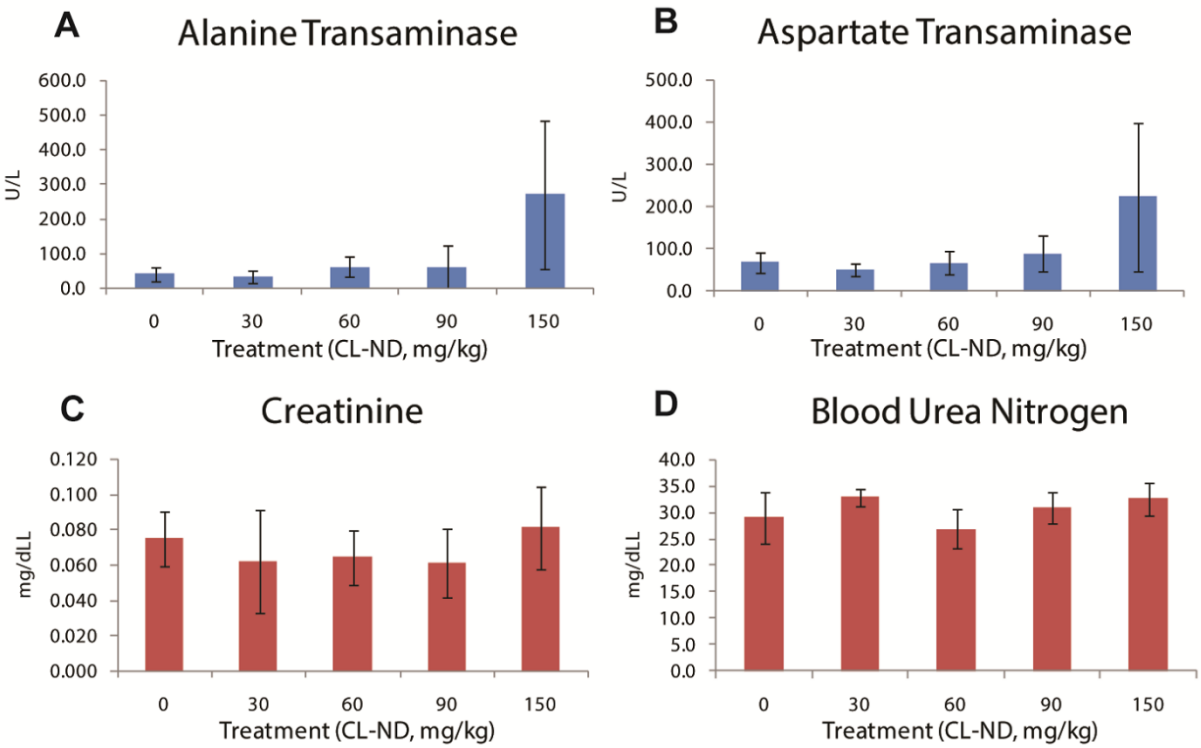

Figure 1. Effect of CL-ND administration on liver and kidney toxicity. WT C57BL/6J mice were injected with escalating doses of CL-ND. Twenty-four h after CL-ND administration, blood was collected and plasma analyzed for liver enzyme (ALT and AST) activity. Kidney toxicity was evaluated by measuring plasma levels of creatinine, and blood urea nitrogen. Results are reported as mean +/- SEM (n = 5).

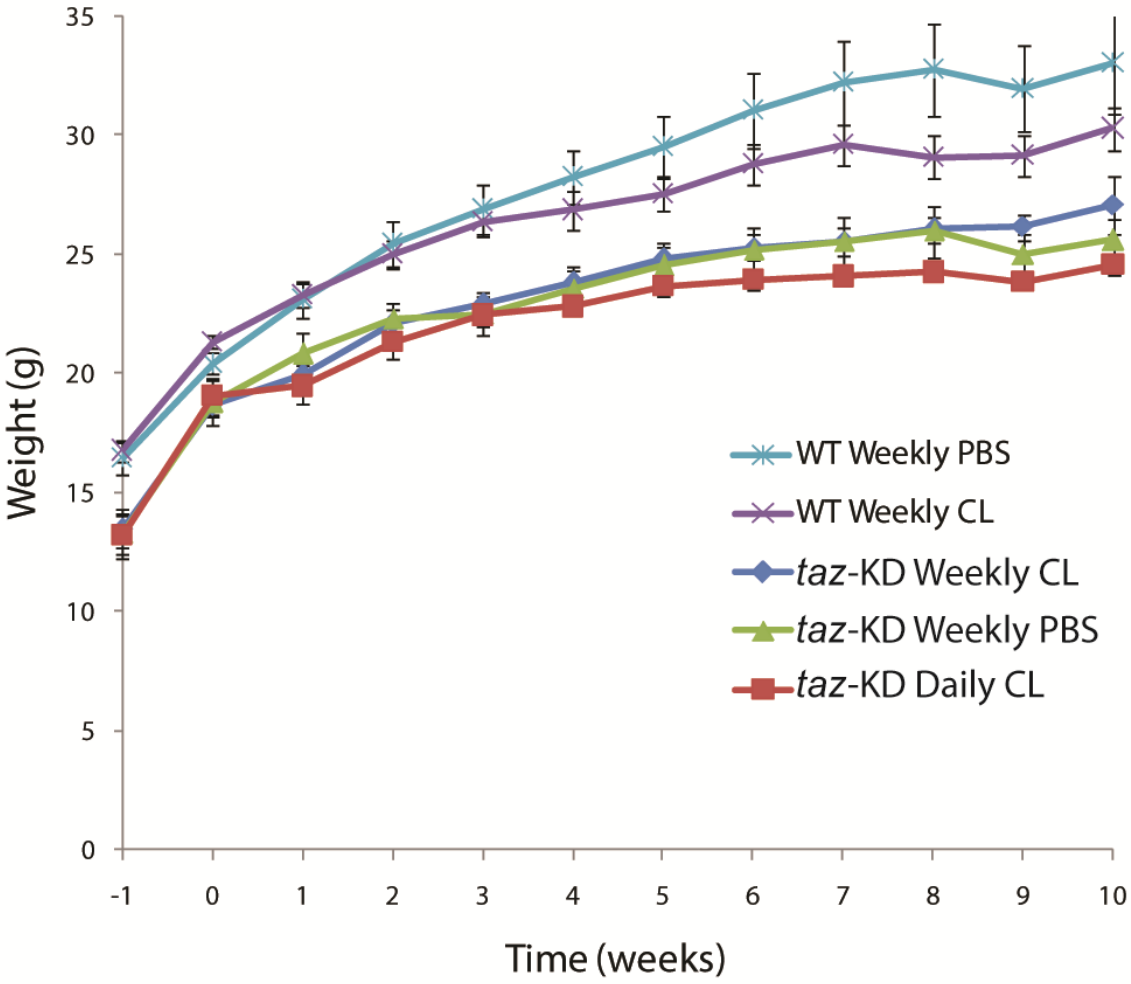

Figure 2. Effect of CL-ND administration on mouse weight gain. Mice were weighed upon arrival (week -1) and every week thereafter until the conclusion of the experiment. Results are reported as mean +/- SEM.

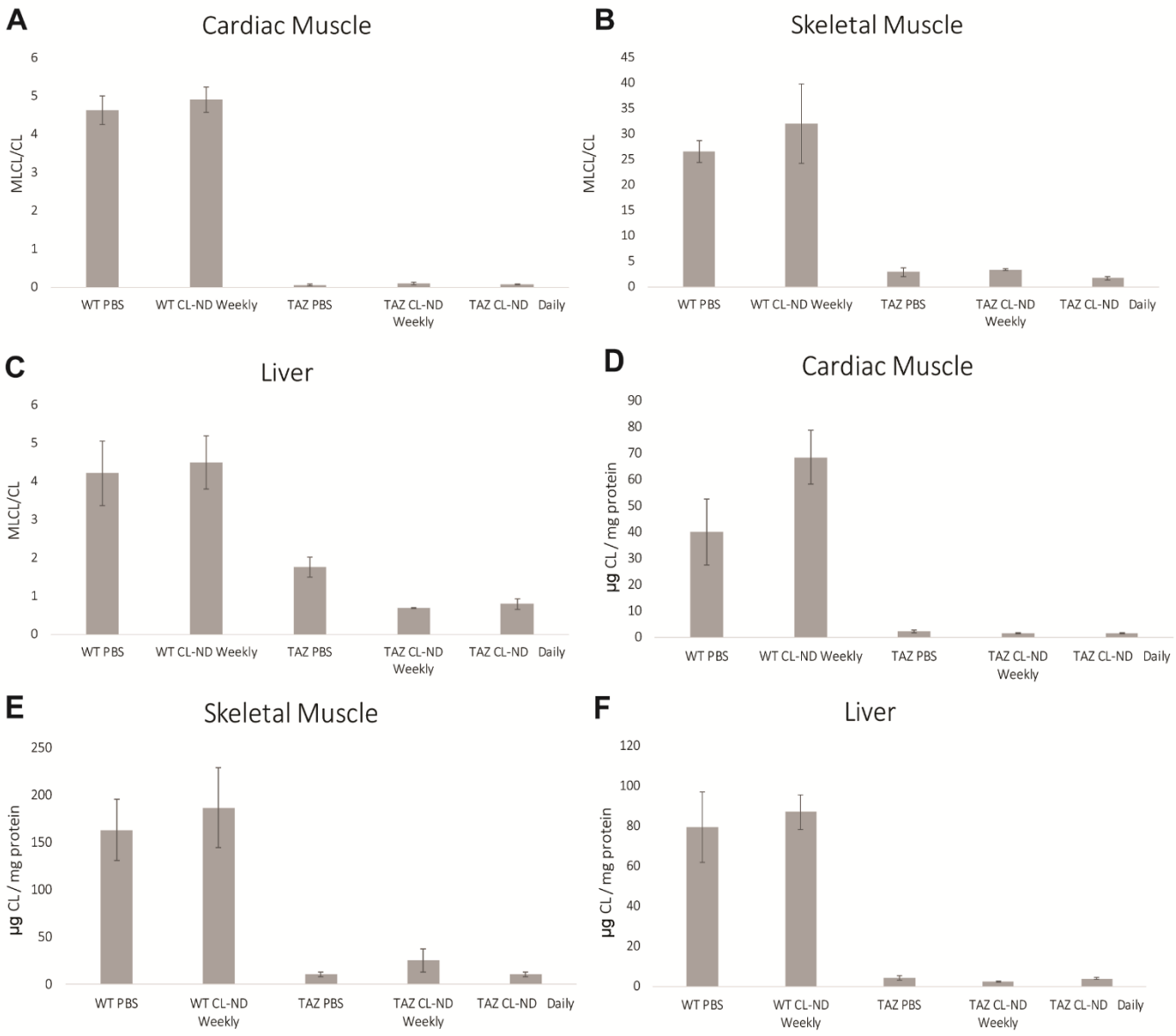

Figure 3. Cardiolipin analysis. At the end of the treatment period, organs were harvested, homogenized, and subject to lipid extraction. The ratio of tetralinoleoyl CL to trilinoleoyl MLCL (CL/MLCL) was quantified by LC/MS (A-C). The absolute amount of tetralinoleoyl CL was quantified relative to an internal standard (D-F). Data are presented as mean +/- SEM.

References

[1] Clarke SL, Bowron A, Gonzalez IL, et al. (2013) Barth syndrome. Orphanet J. Rare Dis. 8; 23.

[2] Bione S, D'Adamo P, Maestrini E, Gedeon AK, Bolhuis PA, Toniolo D. (1996) A novel X-linked gene, G4.5. is responsible for Barth syndrome. Nat. Genet. 12; 385-9.

[3] Whited K, Baile MG, Currier P, Claypool SM (2013) Seven functional classes of Barth syndrome mutation. Hum. Mol. Genet. 22, 483-492.

[4] Xu Y, Malhotra A, Ren M, Schlame M (2006) The enzymatic function of tafazzin. J. Biol. Chem. 281; 39217-39224.

[5] Valianpour F, Mitsakos V, Schlemmer D, et al. (2005) Monolysocardiolipins accumulate in Barth syndrome but do not lead to enhanced apoptosis. J. Lipid Res. 46; 1182-1195.

[6] Ikon, N and Ryan, RO (2017) Cardiolipin and mitochondrial cristae organization. BBA Biomembranes. 1859, 1156-1163.

[7] Bissler JJ, Tsoras M, Goring HH, et al. (2002) Infantile dilated X-linked cardiomyopathy, G4.5 mutations, altered lipids, and ultrastructural malformations of mitochondria in heart, liver, and skeletal muscle. Lab Invest. 82; 335-344.

[8] Ferri L, Donati MA, Funghini S, Malvagia S, Catarzi S, Lugli L, Ragni L, Bertini E, Vaz FM, Cooper DN, Guerrini R, Morrone A. (2013) New clinical and molecular insights on Barth syndrome. Orphanet J. Rare Dis. 8; 27.

[9] Houtkooper RH, Vaz FM. (2008) Cardiolipin, the heart of mitochondrial metabolism. Cell Mol. Life Sci. 65; 2493-2506.

[10] Schlame M, Ren M (2006) Barth syndrome, a human disorder of cardiolipin metabolism] FEBS Lett. 580; 5450-5455.

[11] Valianpour F, Wanders RJ, Overmars H, Vaz FM, Barth PG, van Gennip AH. (2003) Linoleic acid supplementation of Barth syndrome fibroblasts restores cardiolipin levels: implications for treatment. J. Lipid Res. 44; 560-566.

[12] Makaryan V, Kulik W, Vaz FM (2012) The cellular and molecular mechanisms for neutropenia in Barth syndrome. Eur. J. haematol. 88: 195-209.

[13] Ryan, R.O. (2008) Nanodisks: hydrophobic drug delivery vehicle. Expert Opin. Drug Deliv. 5, 343-351.

[14] Ryan, RO (2010) Nanobiotechnology applications of reconstituted high density lipoprotein. J. Nanobiotechnology. 8; 28.

[15] Ikon, N, Su, B, Hsu, F, Forte, TM and Ryan, RO (2015) Exogenous cardiolipin localizes to mitochondria and prevents TAZ knockdown-induced apoptosis in myeloid progenitor cells. Biochem. Biophys. Res. Commun. 464, 580-585.

[16] Acehan D, Vaz F, Houtkooper RH, James J, Moore V, Tokunaga C, Kulik W,

Wansapura J, Toth MJ, Strauss A, Khuchua Z. (2011) Cardiac and skeletal muscle defects in a mouse model of human Barth syndrome. J. Biol. Chem. 286; 899-908.

[17] Soustek MS, Falk DJ, Mah CS, Toth MJ, Schlame M, Lewin AS, Byrne BJ (2011) Characterization of a transgenic short hairpin RNA-induced murine model of Tafazzin deficiency. Hum. Gene Ther. 22; 865-871.

[18] Phoon CK, Acehan D, Schlame M, Stokes DL, Edelman-Novemsky I, Yu D, Xu Y, Viswanathan N, Ren M (2012) Tafazzin knockdown in mice leads to a developmental cardiomyopathy with early diastolic dysfunction preceding myocardial noncompaction. J. Am. Heart Assoc. 1:jah3-e000455 doi: 10.1161/JAHA.111.000455

[19] Ryan, RO, Forte, TM, Oda, MN (2003) Optimizing bacterial expression of human apolipoprotein A-I. Protein Expr. Purif. 27; 98-103.

[20] Hsu FF, Turk J, Rhoades ER, Russell DG, Shi Y, Groisman EA. (2005) Structural characterization of cardiolipin by tandem quadrupole and multiple-stage quadrupole ion-trap mass spectrometry with electrospray ionization. J. Am. Soc. Mass Spectrom. 16; 491-504.

[21] Hsu FF, Turk J. (2006a) Characterization of cardiolipin as the sodiated ions by positive-ion electrospray ionization with multiple stage quadrupole ion-trap mass spectrometry. J. Am. Soc. Mass Spectrom. 17; 1146-1157.

[22] Hsu FF, Turk J. (2006b) Characterization of cardiolipin from Escherichia coli by electrospray ionization with multiple stage quadrupole ion-trap mass spectrometric analysis of [M - 2H + Na]- ions. J. Am. Soc. Mass Spectrom. 17; 420-429.

[23] Hsu FF, Turk J (2008) Toward total structural analysis of cardiolipins: multiple-stage linear ion-trap mass spectrometry on the [M - 2H + 3Li]+ ions. J. Am. Soc. Mass Spectrom. 21; 1863-1869.